

When gold is not enough: platinum standard of quantum chemistry with N^7 cost

Michał Lesiuk*

Faculty of Chemistry, University of Warsaw

Pasteura 1, 02-093 Warsaw, Poland

E-mail: m.lesiuk@uw.edu.pl

Abstract

In this paper we extend the rank-reduced coupled-cluster formalism to the calculation of non-iterative energy corrections due to quadruple excitations. There are two major components of the proposed formalism. The first is an approximate compression of the quadruple excitation amplitudes using the Tucker format. The second is a modified functional used for evaluation of the corrections which gives exactly the same results for the exact amplitudes, but is less susceptible to errors resulting from the aforementioned compression. We show, both theoretically and numerically, that the computational cost of the proposed method scales as the seventh power of the system size. Using reference results for a set of small molecules, the method is calibrated to deliver relative accuracy of a few percent in energy corrections. To illustrate the potential of the theory we calculate the isomerization energy of *ortho/meta* benzyne (C_6H_4) and the barrier height for the Cope rearrangement in bullvalene ($C_{10}H_{10}$). The method retains a near-black-box nature of the conventional coupled-cluster formalism and depends on only one additional parameter that controls the accuracy.

1 Introduction

Tensor decomposition has long been an active area of research in the field of applied mathematics, with successful applications in many branches of science, see Ref. 1 for an exhaustive review. In recent years, tensor decomposition techniques have been embraced by the quantum chemistry community, as exemplified by the development of the tensor hypercontraction (THC) format of the electron repulsion integrals.^{2–5} Pioneering applications to electronic structure methods such as MP2, MP3, random-phase approximation and coupled cluster have also been reported.^{6–17} The primary motivation for applying tensor decompositions to quantum-chemical methods are reductions in terms of computational cost and storage requirements. With a proper calibration these benefits are attainable with an insignificant accuracy loss and without compromising the black-box nature of the parent theoretical method. However, we would like to point out that from the point of view of quantum chemistry, there is an additional potential application of tensor decomposition techniques which has been largely untapped thus far. It is related to the interpretative power of such techniques, exploiting the fact that they can automatically extract important information about the system even from a complicated wavefunction Ansätz, with minimal human oversight.¹

The coupled-cluster (CC) theory^{18,19} is a particularly promising candidate for applying tensor decomposition schemes. In all CC variants the wavefunction is parametrized by a set of cluster amplitudes which can be viewed as multi-dimensional tensors with indices referring to the occupied and virtual orbital sets. Storage and manipulation of these tensors constitutes the main bottleneck in CC calculations for large molecular systems. To address this issue we have recently introduced¹⁴ an approximate CC theory including single, double and triple excitations (CCSDT)^{20,21} where the triply-excited amplitudes tensor is represented in the Tucker-3 format.^{22,23} The increased flexibility offered by this decomposition enables to reduce the scaling of the approximate method by a factor quadratic in the system size in comparison with the exact CCSDT. At the same, accuracy levels of up to 0.1 kJ/mol are reachable in typical applications to chemical problems.

Despite these developments are promising, one may argue from a pragmatic standpoint that being able to reproduce the CCSDT results accurately, even at a significantly reduced cost, is not sufficient for general-purpose applications in thermochemistry, chemical kinetics, molecular interactions, etc. In fact, it is well-documented that in some applications the CCSDT method does not improve the accuracy (in relation to FCI) over the “gold standard” CCSD(T) to a degree that would justify the drastic increase in the computational costs.^{24–29} The reason for this counterintuitive behavior is an accidental, yet systematic, cancellation of errors observed at the CCSD(T) level of theory for “well-behaved” systems. There are two major components of the post-CCSD(T) contribution: (i) the correction to due the inexact treatment of triple excitations and (ii) the correction due to the missing quadruple excitations. It turns out that these two components are often of opposite signs and hence a degree of cancellation occurs. The lesson learned is that the quadruple excitations play a significant role in the $\approx 1 \text{ kJ/mol}$ accuracy range and must be included alongside the full treatment of triple excitations to provide a balanced description.

The importance of quadruple excitations in accurate theoretical studies was recognized in the literature a long time ago. Unfortunately, their complete inclusion by means of the full CCSDTQ theory^{30–33} is prohibitive for molecules comprising more than a few atoms, assuming a decent-quality basis set is used. This prompted research into more affordable methods that are able to account for the quadruple excitations in an approximate, yet still reliable, way. Several families of such methods were proposed,^{34–41} both iterative and non-iterative, based either on the ordinary Møller-Plesset perturbation theory or various effective Hamiltonian approaches, and employing either CCSD or CCSDT wavefunctions as the starting point. A more detailed technical discussion of these methods is given in subsequent sections. In this work we concentrate primarily on the CCSDT(Q) theory introduced by Bomble *et al.*³⁷ which has become *de facto* standard in high-accuracy quantum chemical calculations. Due to a good balance between the accuracy and computational costs, it is a member of various composite electronic structure protocols and is implemented in several program packages

available for public use. In many applications, the CCSDT(Q) theory is considered to be the “platinum standard” of quantum chemistry²⁹ – the next rung of the coupled-cluster ladder above CCSD(T) striking a balance between the accuracy and computational costs. Computation of the (Q) correction is usually 1 – 2 orders of magnitude less computationally intensive than the complete CCSDTQ calculations. Despite this drastic reduction, the range of applicability of the CCSDT(Q) theory to polyatomic molecules remains limited as a result of steep N^9 scaling of the computational costs with the system size, N .

This work is a continuation of a series of papers^{11,14,16,17} where tensor decomposition techniques are applied as a tool to reduce the cost of high-order CC methods. In this part, we introduce a rank-reduced approach to computation of the (Q) correction. There are two main distinguishing features of the proposed scheme. The first is the compression of the quadruply-excited amplitudes using the Tucker format which enables to reduce the immense cost of storing and manipulating the T_4 amplitudes. To achieve the necessary transformation from the full rank to rank-reduced representation of the quadruply-excited amplitudes we develop an iterative method based on higher-order orthogonal iteration (HOOI) procedure.^{42,43} The second feature is the development of a modified functional used to evaluate the (Q) correction. Due to the variational nature of this functional, it is less sensitive to the errors incurred by the rank-reduced treatment of the CC amplitudes. This enables to evaluate the (Q) correction with a mean relative accuracy of a few percent. Taking into account that the (Q) method itself is able to recover, on average, about 90% of the CCSDTQ-CCSDT energy difference,⁴⁴ these errors are acceptable from a practical point of view. Critically, by properly factorizing the working expression of the proposed method and exploiting the rank-reduced format of the CC amplitudes, it is possible to evaluate the (Q) correction with the N^7 cost. Finally, we report calculations of relative energies for larger systems, demonstrating a broad range of applicability and reliability of the proposed theory. In particular, we study the isomerization energy of *ortho/meta* benzyne and the Cope rearrangement in bullvalene molecule.

Table 1: Details of the notation adopted in the present work; O is the number of active occupied in the reference, V is the number of virtual orbitals. For convenience of the readers the key defining equations were included in the last column.

Indices	Limit	Corresponds to	Defining equation
i, j, k, l, \dots	O	active occupied orbitals	—
a, b, c, d, \dots	V	unoccupied (virtual) orbitals	—
p, q, r, s, \dots	—	general orbitals	—
P, Q, \dots	N_{aux}	density-fitting basis set	$(pq rs) = B_{pq}^Q B_{rs}^Q$
X, Y, Z, \dots	N_{SVD}	subspace of triply-excited amplitudes	$t_{ijk}^{abc} = t_{XYZ} U_{ai}^X U_{bj}^Y U_{ck}^Z$
A, B, C, \dots	N_{qua}	subspace of quadruply-excited amplitudes	$t_{ijkl}^{abcd} = t_{ABCD} V_{ai}^A V_{bj}^B V_{ck}^C V_{dl}^D$

2 Theory

2.1 Preliminaries

In this work we consider closed-shell systems and employ the canonical restricted Hartree-Fock (HF) determinant, denoted $|\phi_0\rangle$, as the reference wavefunction in the CC theory. The HF orbital energies are denoted by ϵ_p . For brevity, we also introduce the following conventions: $\langle A \rangle \stackrel{\text{def}}{=} \langle \phi_0 | A \phi_0 \rangle$ and $\langle A | B \rangle \stackrel{\text{def}}{=} \langle A \phi_0 | B \phi_0 \rangle$ for arbitrary operators A, B . Unless explicitly stated otherwise, the Einstein convention for summation over repeated indices is employed throughout. The standard partitioning of the electronic Hamiltonian, $H = F + W$, into the sum of the Fock operator (F) and the fluctuation potential (W) is adopted. The remaining aspects of the notation are summarized in Table 1.

The method for evaluation of non-iterative quadruples correction reported in this work builds upon the SVD-CCSDT theory introduced in Ref. 14. The electronic wavefunction underlying the SVD-CCSDT method is given by $|\Psi\rangle = e^{T_{\text{SVD}}} |\phi_0\rangle$ with $T_{\text{SVD}} = T_1 + T_2 + T_3^{\text{SVD}}$. The T_1 and T_2 operators have the same form as in the usual CCSDT theory

$$T_1 = t_i^a E_{ai}, \quad T_2 = \frac{1}{2} t_{ij}^{ab} E_{ai} E_{bj}, \quad (1)$$

where t_i^a , t_{ij}^{ab} are the cluster amplitudes, and $E_{pq} = p_\alpha^\dagger q_\alpha + p_\beta^\dagger q_\beta$ are the spin-adapted singlet orbital replacement operators.⁴⁵ The triply excited component of the cluster operator is approximated as

$$T_3^{\text{SVD}} = \frac{1}{6} t_{ijk}^{abc} E_{ai} E_{bj} E_{ck}, \quad \text{with} \quad t_{ijk}^{abc} \approx t_{XYZ} U_{ai}^X U_{bj}^Y U_{ck}^Z. \quad (2)$$

The quantities U_{ai}^X are obtained by a procedure described in Ref. 17 and are fixed during the coupled-cluster iterations. The remaining unknown quantities (t_i^a , t_{ij}^{ab} , and t_{XYZ}) are found by projecting $e^{-T_{\text{SVD}}} H e^{T_{\text{SVD}}} |\phi_0\rangle = 0$ onto a proper subset of excited determinants, and solving the resulting non-linear equations. The dimension of the compressed amplitudes tensor t_{XYZ} is denoted by N_{SVD} , see Table 1, and it scales linearly with the system size. Note that this tensor is supersymmetric, i.e. invariant to any permutation of the indices X , Y , Z .

As a computationally convenient representation of the electron repulsion integrals we employ the density-fitting approximation^{46–50}

$$(pq|rs) \approx B_{pq}^Q B_{rs}^Q, \quad \text{with} \quad B_{pq}^Q = (pq|P) [\mathbf{V}^{-1/2}]_{PQ}, \quad (3)$$

where $(pq|P)$ and $V_{PQ} = (P|Q)$ are the three-center and two-center electron repulsion integrals, respectively. Because the Coulomb metric is used in Eq. (3) for determination of density-fitting coefficients, this formula is automatically “robust” in the sense that the error in the integrals is quadratic in the density errors.⁴⁸ The capital letters P , Q are employed in the present work for the elements of the auxiliary basis set. The number of auxiliary basis set functions is denoted by the symbol N_{aux} . By construction, N_{aux} scales linearly with the size of the system. In all calculations reported in this work, the error in relative energies caused by the density-fitting approximation was negligible in comparison with other uncertainties. This is consistent with other studies on this topic found in the literature.^{51,52}

2.2 Non-iterative quadruples corrections

The problem of economical inclusion of quadruple excitations effects in the CC theory was first considered by Kucharski, Bartlett and collaborators.^{34–36,53–56} They introduced a non-iterative method, denoted CCSDT[Q] or simply [Q] in the present work, based on the standard Møller-Plesset perturbation theory where the Hartree-Fock determinant serves the role of the zeroth-order wavefunction. The quadruple excitation cluster operator T_4 is obtained from an approximate formula

$$\langle \mu_4 | [F, T_4] + [W, T_3] + \frac{1}{2} [[W, T_2], T_2] \rangle = 0, \quad (4)$$

where μ_4 stands for an appropriate string of quadruple excitation operators, i.e. $\mu_4 = E_{ai} E_{bj} E_{ck} E_{dl}$, and hence $\langle \mu_4 |$ denotes projection onto the quadruply-excited configurations. A similar notation is used below also for lower-order excitations, e.g. $\mu_3 = E_{ai} E_{bj} E_{ck}$. As the Fock operator is diagonal in the canonical orbital basis, Eq. (4) can be explicitly solved to get the quadruply excited amplitudes in a closed-form

$$t_{ijkl}^{abcd} = (\epsilon_{ijkl}^{abcd})^{-1} \langle \mu_4 | [W, T_3] + \frac{1}{2} [[W, T_2], T_2] \rangle, \quad (5)$$

where $\epsilon_{ijkl}^{abcd} = \epsilon_i + \epsilon_j + \epsilon_k + \epsilon_l - \epsilon_a - \epsilon_b - \epsilon_c - \epsilon_d$ is the four-particle energy denominator. The CCSDT[Q] correction to the energy (abbreviated as $E_{[Q]}$) originating from the missing quadruple excitations then reads

$$E_{[Q]} \equiv E_{[Q]}^{[5]} = \langle T_2 | [W, T_4] \rangle, \quad (6)$$

where the superscript [5] indicates that the term enters in the fifth order of the Møller-Plesset perturbation theory. An alternative method to account for the quadruple excitations was presented by Bomble *et al.*³⁷ who employed Löwdin's partitioning of the coupled-cluster EOM Hamiltonian.⁵⁷ This method is nowadays most commonly referred to as CCSDT(Q).

The main difference between this approach and the pioneering developments of Kucharski and Bartlett is that the CCSDT wavefunction, rather than the Hartree-Fock determinant, is employed as zeroth-order wavefunction. The resulting energy correction, denoted by $E_{(Q)}$, uses the same formula (5) for the quadruply-excited amplitudes, but is given by sum of two terms

$$E_{(Q)} = E_Q^{[5]} + E_Q^{[6]}. \quad (7)$$

The former term is the same as in the CCSDT[Q] method, Eq. (6), while the latter reads

$$E_Q^{[6]} = \langle T_3 | [W, T_4] \rangle. \quad (8)$$

As suggested by the notation, the term $E_Q^{[6]}$ is of the sixth order in the usual perturbation theory and hence it was neglected in the CCSDT[Q] method. However, it has been shown³⁷ that the importance of the $E_Q^{[6]}$ contribution is much larger than its formal order would suggest. Only in the basis sets of double-zeta quality the term $E_Q^{[5]}$ is dominating and the contribution from $E_Q^{[6]}$ is typically smaller by an order of magnitude. This changes when the size of the basis set is increased to triple-zeta or larger. The terms $E_Q^{[5]}$ and $E_Q^{[6]}$ are then of a similar magnitude, with the latter even becoming dominant in some cases. As an immediate consequence, relative accuracy of the CCSDT[Q] method (in comparison to CCSDTQ) deteriorates with increasing basis set size. The accuracy level of the (Q) correction, on the other hand, was found to be remarkably consistent at least up to quintuple-zeta basis sets.³⁷ In the present work we concentrate primarily on the implementation of the CCSDT(Q) method as a way of incorporating the effects of quadrupole excitations into the rank-reduced CC formalism. To further justify this choice, below we provide a short survey of other available methods. We concentrate on closed-shell systems and hence open-shell generalizations are not discussed.

In the factorizable [Q] method,³⁵ denoted accordingly by $[Q_f]$, one employs the factor-

ization theorem⁵⁸ to get rid of the four-particle denominator in evaluation of the $E_Q^{[5]}$ term. While this factorization is only approximate in the case of CCSDT amplitudes entering Eq. (6), the quality of this approximation is usually excellent. The main advantage of the $[Q_f]$ method is the reduced scaling of the computational cost with the system size. While the exact computation of the $[Q]$ correction scales as N^9 , evaluation of the factorizable variant $[Q_f]$ can be accomplished with the N^7 cost. Unfortunately, the $[Q_f]$ method itself is an approximation to the $[Q]$ correction, and hence it is bound to suffer from the same basis set dependency problems. To the best of our knowledge, analogous factorization cannot be accomplished for the $E_Q^{[6]}$ term that involves projection onto the triply excited amplitudes.

The second family of non-iterative quadruples corrections retains different parametrization of the left- and right-hand-side coupled-cluster wavefunctions.³⁸ The resulting CCSDT $[Q]_\Lambda$ and CCSDT(Q) $_\Lambda$ methods offer a noticeable improvement in terms of the accuracy in comparison to their conventional counterparts described above. However, this comes at a cost of evaluating the so-called coupled-cluster Lagrangian which is not available at present for the rank-reduced CCSDT method and requires a separate study. Next, we discuss the recently introduced CCSDT(Q - n) family of methods derived from Lagrangian-based perturbation theory, treating CCSDT as the zeroth-order wavefunction.^{40,41} This framework is free from size-inconsistency problems encountered in the preceding EOM-like approaches and has been shown to converge rapidly to the exact CCSDTQ limit. While CCSDT(Q -2) is not competitive with the CCSDT(Q) theory, the improved CCSDT(Q -3) variant offers an excellent accuracy level.⁴⁴ Unfortunately, the computational cost of CCSDT(Q -3) method is comparable to a single CCSDTQ iteration (N^{10} scaling) and hence it is beyond the scope of the present work. Last but not least, the renormalized and completely renormalized approaches developed by Piecuch and collaborators⁵⁹⁻⁶² are derived using the so-called CC method of moments. They drastically improve the accuracy for systems with significant multireference character, but for systems dominated by a single reference determinant the results are similar.

2.3 Quadratic (Q) functional: exact formulation

In the rank-reduced context, the formulation of the (Q) correction based on Eqs. (6), (7), and (8) has a significant disadvantage. It stems from the fact that these equations were derived assuming that the T_1 , T_2 , and T_3 amplitudes come from the exact CCSDT theory, and T_4 amplitudes are obtained by solving Eq. (4) without further approximations. In the rank-reduced formalism these assumptions do not hold; for example, the T_3 amplitudes are subject to the Tucker-3 compression, see Eq. (2). Unfortunately, if approximate cluster amplitudes are used to evaluate Eqs. (6) and (8), the error in the (Q) correction is roughly proportional to the error of the amplitudes. In other words, there exists an approximate linear relationship connecting the average error in the amplitudes and the error in the (Q) correction. To avoid this problem and to guarantee that the latter error vanishes more rapidly as the accuracy of the amplitudes is improved, we propose a different functional for evaluation of the (Q) correction. The general form of the new functional, denoted $\mathcal{L}_{(Q)}$ further in the text, reads

$$\begin{aligned} \mathcal{L}_{(Q)} = & \langle T_2 | [W, T_4] \rangle + \langle T_3 | [W, T_4] \rangle + \langle L_3 | e^{-T} H e^T \rangle \\ & + \langle L_4 | [F, T_4] + [W, T_3] + \frac{1}{2} [[W, T_2], T_2] \rangle. \end{aligned} \quad (9)$$

where L_3 and L_4 are two new auxiliary operators which assume the standard form

$$L_3 = \frac{1}{6} l_{ijk}^{abc} \mu_3, \quad \text{and} \quad L_4 = \frac{1}{24} l_{ijkl}^{abcd} \mu_4, \quad (10)$$

and the new amplitudes l_{ijk}^{abc} and l_{ijkl}^{abcd} are yet to be determined. The proposed functional has to fulfill two main theoretical requirements in order to be useful in the rank-reduced context:

- if the exact CCSDT amplitudes together with T_4 amplitudes calculated from Eq. (4) are used, the new functional gives *strictly* identical results as the original formulation based on Eqs. (6) and (8);

- the error of the (Q) correction evaluated using the new functional is quadratic in the error of the T_3/L_3 and T_4/L_4 amplitudes.

The motivation behind the first requirement is to enforce that in the limit of the complete triple excitation subspace in Eq. (2), i.e. when the SVD-CCSDT method is equivalent to the conventional CCSDT, the exact (Q) correction is recovered. Regarding the second requirement, the goal is to reduce the impact of the approximations adopted in the treatment of T_3 and T_4 amplitudes on the accuracy of the (Q) correction. However, one might ask why the quadratic error property is enforced only with respect to the T_3 and T_4 amplitudes, disregarding the T_2 amplitudes that enter Eq. (6) directly and Eq. (8) indirectly *via* the T_4 operator. The justification is purely pragmatic and is based on a numerical observation that the T_2 amplitudes obtained from SVD-CCSDT method are sufficiently accurate for the purposes of evaluating Eqs. (6) and (8). In fact, we verified that even the use of CCSD T_2 amplitudes results in acceptable errors. This finding is not entirely surprising as similar arguments are used in the derivation of the aforementioned factorizable approximation to the $E_Q^{[5]}$ term. All in all, while the second requirement given above can be strengthened to include the T_2 amplitudes as well, we found no practical reason to justify such choice, taking into account the increased complexity of the resulting formalism.

It is straightforward to verify that for any L_3 and L_4 operators, the $\mathcal{L}_{(Q)}$ functional automatically fulfills the first requirement given in the previous paragraph. In fact, when the exact CCSDT amplitudes are inserted into the above formula, the third term vanishes identically as a consequence of the CCSDT stationary condition for the triple excitation amplitudes, $\langle \mu_3 | e^{-T} H e^T \rangle = 0$. Similarly, if the T_4 amplitudes are determined from Eq. (4) without approximations, the fourth term included in $\mathcal{L}_{(Q)}$ also vanishes, as it is a projection of Eq. (4) onto some set of L_4 amplitudes.

In order to satisfy the second requirement discussed above, we demand that the $\mathcal{L}_{(Q)}$ functional is stationary with respect to variations in the T_3 , T_4 , L_3 , and L_4 amplitudes. In other words, we impose a condition that the first derivative of Eq. (9) with respect to each of

these amplitudes separately is zero. Differentiation with respect to the L_3 and L_4 amplitudes returns back the stationary conditions and Eq. (4), respectively, and hence this brings no new information into the formalism. By differentiating $\mathcal{L}_{(Q)}$ with respect to the T_3 and T_4 amplitudes, respectively, and setting the resulting equations to zero one obtains

$$\langle \mu_3 | [W, T_4] \rangle + \langle L_3 | [e^{-T} H e^T, \mu_3] \rangle + \langle L_4 | [W, \mu_3] \rangle = 0, \quad (11)$$

and

$$\langle T_2 | [W, \mu_4] \rangle + \langle T_3 | [W, \mu_4] \rangle + \langle L_4 | [F, \mu_4] \rangle = 0, \quad (12)$$

respectively. The latter equation can be directly solved to obtain the L_4 amplitudes. Upon inserting the results into Eq. (11), it becomes a system of linear equations with the L_3 amplitudes being the only unknowns. Therefore, Eqs. (11) and (12) completely determine the auxiliary L_3 and L_4 operators, and hence enable calculation of the modified (Q) functional, Eq. (9).

With Eqs. (11) and (12) at hand, it remains to show that the quantity $\mathcal{L}_{(Q)}$ indeed fulfills the second condition discussed above. The simplest way to achieve this is to employ the chain rule of differentiation and exploit the stationary conditions (9). However, in Supporting Information we provide a more detailed derivation that has the advantage of providing a rigorous error estimation, namely

$$\delta \mathcal{L}_{(Q)} = \langle \delta T_3 | [W, \delta T_4] \rangle + \langle \delta L_3 | [e^{-T^{\text{ex}}} H e^{T^{\text{ex}}}, \delta T_3] \rangle + \langle \delta L_4 | [F, \delta T_4] + [W, \delta T_3] \rangle, \quad (13)$$

where T^{ex} denotes the exact CCSDT amplitudes, while δT_3 is an error in the T_3 operator (analogous notation is used for the remaining quantities). It is straightforward to verify that each term of the above formula is quadratic in the combined powers of δT_3 , δL_3 , δT_4 , and δL_4 . This proves that the proposed functional $\mathcal{L}_{(Q)}$ satisfies the second requirement

introduced at the beginning of this section.

2.4 Quadratic (Q) functional: approximations

In order to make calculations based on the quadratic (Q) functional feasible, approximations need to be introduced to the exact formalism presented in the previous section. However, we stress that in order to retain the desirable properties of the $\mathcal{L}_{(Q)}$ functional, no approximations are made to its formal definition given by Eq. (9). Instead, we adopt several simplifications to the equations that determine the T_3 , T_4 , L_4 , and L_3 operators, as described in detail in this section. Due to the quadratic nature of the $\mathcal{L}_{(Q)}$ functional, these approximations are expected to have a small impact on the accuracy of the (Q) correction.

Starting with the T_3 operator, it is given by the approximate form (2), inherited after the SVD-CCSDT theory, with the amplitudes compressed using the Tucker-3 format. We adopt no further approximations to this quantity.

Moving to the T_4 operator, the handling and storage of the full-rank quadruply-excited amplitudes given by Eq. (5) constitutes the major bottleneck of the exact formalism. To overcome this obstacle we approximately cast the quadruply-excited amplitudes (5) in a rank-reduced form employing the Tucker format

$$t_{ijkl}^{abcd} \approx t_{ABCD} V_{ai}^A V_{bj}^B V_{ck}^C V_{dl}^D, \quad (14)$$

which is fully analogous to the rank-reduced form of the triply-excited amplitudes, cf. Eq. (2). As the expansion basis vectors V_{ai}^A are distinct from their counterparts used in Eq. (2), we employ the capital letters A, B, C, \dots to denote the quantities that relate to the quadruply-excited amplitudes. The dimension of the core tensor t_{ABCD} in Eq. (14) is referred to as N_{qua} . By analogy with the findings for the doubly- and triply-excited amplitudes represented in the Tucker- n format, we assume that N_{qua} scales linearly with the system size. A numerical demonstration of this condition is presented in Sec. 3.2. The conversion of

the full-rank quadruply-excited amplitudes t_{ijkl}^{abcd} to the compressed form (14) is non-trivial. To accomplish this task we propose a novel algorithm based on higher-order orthogonal iteration (HOOI). Details of this procedure are described in the next section, along with the analysis of the computational costs and scaling with the system size.

Next, we consider the auxiliary operator L_4 which is defined by Eq. (12). To facilitate efficient evaluation of this quantity, we adopt two levels of approximatiofns. First, in Eq. (12) we neglect the term that involves the triply excited amplitudes, namely $\langle T_3 | [W, \mu_4] \rangle$. The justification of this approximation is rooted in the standard Møller-Plesset perturbation theory, where the T_2 operator enters in the first-order perturbed wavefunction, while the T_3 operator appears in the second order. By the same token, we expect the contribution of the $\langle T_2 | [W, \mu_4] \rangle$ to be dominating, while the neglected term constitutes a relatively minor correction. The neglect of the term $\langle T_3 | [W, \mu_4] \rangle$ leads to the modified expression

$$\langle T_2 | [W, \mu_4] \rangle + \langle L_4 | [F, \mu_4] \rangle = 0, \quad (15)$$

which can easily be solved directly by exploiting the diagonal nature of the canonical Fock operator, giving

$$l_{ijkl}^{abcd} = (\epsilon_{ijkl}^{abcd})^{-1} \langle \mu_4 | W T_2 \rangle. \quad (16)$$

In Supporting Information we provide an explicit formula for this quantity expressed through the basic CC amplitudes and two-electron integrals. The second level of approximation adopted for L_4 is the same as for the T_4 , i.e. rank-reduction to the Tucker-4 format

$$l_{ijkl}^{abcd} \approx l_{A'B'C'D'} V_{ai}^{A'} V_{bj}^{B'} V_{ck}^{C'} V_{dl}^{D'}, \quad (17)$$

where the primes have been added to underline that the expansion basis is different from that of Eq. (14). Similarly as for the T_4 operator, in the next section we provide technical

details of the HOOI procedure used to determine the rank-reduced L_4 amplitudes.

Finally, let us consider the L_3 operator for which the approximation scheme is somewhat more involved and consists of two steps. In the first step, we neglect the fluctuation potential W in the similarity-transformed Hamiltonian present in Eq. (11) and set $e^{-T}H e^T \approx e^{-T}F e^T$. This leads to the modified formula

$$\langle \mu_3 | [W, T_4] \rangle + \langle L_3 | [F, \mu_3] \rangle + \langle L_4 | [W, \mu_3] \rangle = 0, \quad (18)$$

where we have additionally exploited the fact that $[e^{-T}F e^T, \mu_3] = [F, \mu_3]$ which is straightforward to prove using the BCH expansion. By exploiting the properties of the Fock operator, explicit solution of this equation is written as

$$l_{ijk}^{abc} = (\epsilon_{ijk}^{abc})^{-1} \langle \mu_3 | [W, T_4 + L_4] \rangle, \quad (19)$$

where the equality $\langle L_4 | [W, \mu_3] \rangle = \langle \mu_3 | [W, L_4] \rangle$ has been used for convenience sake.

To introduce the second layer of approximation, we note that the third term in Eq. (18) is dominating in comparison with the first term. This is again justified by perturbation theory arguments; by comparing Eqs. (15) and (4) we see that L_4 is a second-order quantity, while T_4 is a third-order quantity. Therefore, it is tempting to neglect the $\langle \mu_3 | [W, T_4] \rangle$ term altogether in Eq. (18), in a similar spirit as in the previous paragraph where approximations of the L_4 operator were discussed. We considered this approach in the preliminary stage of the implementation and verified that it indeed delivers a decent accuracy level. However, there exists an alternative approach to approximating the L_3 operator which is based on the Tucker format

$$l_{ijk}^{abc} \approx l_{X'Y'Z'} U_{ai}^{X'} U_{bj}^{Y'} U_{ck}^{Z'}, \quad (20)$$

where the primes indicate that the quantities $U_{ai}^{X'}$ are distinct from the expansion basis used

for the triply-excited amplitudes in Eq. (2). Similarly as for other quantities, HOOI is used to bring l_{ijk}^{abc} into the decomposed form (20). However, as a cost-saving measure, we introduce a simplification: the expansion basis $U_{ai}^{X'}$ is found by decomposing an approximate form of the l_{ijk}^{abc} , namely

$$l_{ijk}^{abc} \approx (\epsilon_{ijk}^{abc})^{-1} \langle \mu_3 | [W, L_4] \rangle, \quad (21)$$

where the term including the T_4 operator has been neglected, cf. Eq. (19). Once the quantities $U_{ai}^{X'}$ are found, the core tensor $l_{X'Y'Z'}$ is found by projection:

$$l_{X'Y'Z'} = (\epsilon_{ijk}^{abc})^{-1} \langle \mu_3 | [W, T_4 + L_4] \rangle U_{ai}^{X'} U_{bj}^{Y'} U_{ck}^{Z'}. \quad (22)$$

Note that in this step the full form of the L_3 operator is used, without any approximations in comparison with Eq. (19). We found that this hybrid approach reduces the computational cost of decomposing the amplitudes l_{ijk}^{abc} considerably without affecting the accuracy of the decomposition (20). This can be explained by noting that the term involving the T_4 is numerically minor. Therefore, the basis found using the decomposition of the approximate formula, Eq. (20), is able to accommodate both terms accurately, despite the T_4 is absent in the optimization procedure.

To study the impact of the proposed approximations, we carried out calculations for small molecular systems from Sec. 3.3. In Supporting Information we provide detailed results for the most representative case using the cc-pVDZ, cc-pVTZ, and cc-pVQZ basis sets. These data show that the neglected terms are numerically small and some additional approximations proposed above have a small impact on the accuracy of the proposed formalism.

Finally, let us point out that, in general, the dimensions of the quadruple excitation subspace (N_{qua}) used for compression of the t_{ijkl}^{abcd} and l_{ijkl}^{abcd} amplitudes, i.e. in Eqs. (14) and (17), can be different. Similarly, different sizes of the triple excitation subspace (N_{SVD}) may be used for T_3 and L_3 operators. However, in a set of preliminary calculations we

found that near-optimal results are attained when the same size of the quadruple excitation subspace is used for T_4 and L_4 , and the same size of triple excitation subspace for T_3 and L_3 . Therefore, we use a single parameter N_{qua} to denote the length of the expansion in both Eq. (14) and (17), and similarly N_{SVD} for both Eq. (20) and (2). Gains in terms of accuracy achieved by lifting these restrictions do not justify the corresponding increase of the technical complexity of the formalism.

2.5 Compression of the excitation amplitudes

As mentioned in the previous section, the decomposition of the triply- and quadruply-excited amplitudes, required to evaluate the approximate form of the quadratic functional detailed in Sec. 2.4, is achieved using the higher-order orthogonal iteration (HOOI) procedure. In this section we provide details of this procedure, both theoretical and technical. We concentrate primarily on the decomposition of the t_{ijkl}^{abcd} tensor as this is the most problematic quantity. However, extension of this procedure to the amplitudes present in the L_3 and L_4 operators is briefly discussed at the end of the present section, and further technical details are presented in Supporting Information.

In the HOOI procedure the decomposition of the amplitudes is achieved by minimization of the following cost function

$$\sum_{ijkl} \sum_{abcd} \left[t_{ijkl}^{abcd} - t_{ABCD} V_{ai}^A V_{bj}^B V_{ck}^C V_{dl}^D \right]^2, \quad (23)$$

subject to the condition that the V_{ai}^A vectors are column orthonormal, that is

$$V_{ai}^A V_{ai}^B = \delta_{AB}. \quad (24)$$

The constraint (24) is imposed without loss of generality, because any linear transformation amongst the V_{ai}^A vectors can be counteracted by changing the values of the core tensor,

leaving the cost function unaffected. For a fixed expansion length (N_{qua}) the least-squares problem (23) is solved by HOOI which in the present case proceeds as follows. Assuming that an approximate solution V_{ai}^A of the minimization problem (23) is known, one forms an intermediate quantity

$$t_{ai,BCD} = t_{ijkl}^{abcd} V_{bj}^B V_{ck}^C V_{dl}^D, \quad (25)$$

which is a partial projection of the full-rank tensor onto the current subspace. Next, the truncated singular value decomposition (SVD) of the $t_{ai,BCD}$ tensor is computed. The left-singular vectors corresponding to N_{qua} the largest singular values form the updated expansion vectors, V_{ai}^A . Note that by the virtues of the SVD procedure the new vectors automatically obey the orthonormality constraint (24). This basic iteration process is repeated until the convergence criterion is met; a convenient choice of the stopping criteria is discussed further in the text. Note that during the HOOI procedure the core tensor t_{ABCD} does not have to be formed explicitly. Nonetheless, it is obtained straightforwardly as

$$t_{ABCD} = t_{ai,BCD} V_{ai}^A, \quad (26)$$

owing to the orthonormality of the expansion vectors, V_{ai}^A .

The basic HOOI procedure described above constitutes a serviceable method. Unfortunately, due to large dimensions of the $t_{ai,BCD}$ matrix, namely $OV \times N_{\text{qua}}^3$, the SVD step of this algorithm is too expensive for large-scale applications. Therefore, we introduce a modification of the HOOI procedure where instead of the $t_{ai,BCD}$ matrix the following quantity is computed

$$M_{ai,bj} = t_{ai,BCD} t_{bj,BCD}. \quad (27)$$

Let us recall that for any rectangular matrix \mathbf{M} , its left singular-vectors coincide with the

eigenvectors of the normal matrix $\mathbf{M}\mathbf{M}^T$. Therefore, the updated expansion vectors V_{ai}^A can equivalently be obtained by diagonalizing the $M_{ai,bj}$ matrix and retaining the eigenvectors corresponding to the largest eigenvalues (which are non-negative by construction). The dimensions of the $M_{ai,bj}$ matrix are $OV \times OV$ and hence it admits eigendecomposition in N^6 time, a significant improvement over the SVD of the $t_{ai,BCD}$ matrix. As a by-product, the modification of the HOOI procedure described above solves the memory bottleneck related to the storage of the complete $t_{ai,BCD}$ matrix (N^5 memory chunk). In our implementation, the $t_{ai,BCD}$ matrix is calculated in batches with one of the B, C, D indices fixed. The batches are then immediately used to compute the contribution to $M_{ai,bj}$ without accumulation of the full $t_{ai,BCD}$ matrix. The storage requirements are reduced in this way to the level of $OVN_{\text{qua}}^2 \propto N^4$.

It remains to discuss two technical aspects of the HOOI algorithm, i.e., the choice of the stopping criteria and the starting values. As discussed at length in Ref. 17 an appropriate stopping condition is obtained by monitoring the norm of the core tensor

$$\|t\|^2 = \sum_{ABCD} t_{ABCD}^2 = \sum_A M_{ai,bj} V_{ai}^A V_{bj}^A, \quad (28)$$

where the second equality follows from the orthonormality of the V_{ai}^A vectors. The HOOI procedure is ended when the relative difference in $\|t\|$ between two consecutive iterations falls below a predefined threshold, ϵ . The threshold value of $\epsilon = 10^{-6}$ is sufficient in most applications and has been adopted in the present work. The cost of computing $\|t\|$ is negligible in comparison with other parts of the algorithm. The reason why this straightforward procedure performs well in practice is a consequence of the fact that the HOOI algorithm can be reformulated as a maximization of the norm of the core tensor instead of minimization of Eq. (23), see Refs. 42,63.

The problem of the starting values is solved simply by setting V_{ai}^A as equal to U_{ai}^X that correspond to the largest absolute diagonal values of t_{XYZ} , see Eq. (2). We found this

procedure to be entirely satisfactory in practice and convergence of the HOOI procedure is achieved typically within only $5 - 10$ iterations to accuracy of $\epsilon = 10^{-6}$. The sole exception from this rule occurs in calculations with extremely small N_{qua} , but it is questionable whether they are of any practical importance. The major steps of the HOOI algorithm are summarized in Algorithm 1.

Algorithm 1: Pseudo-code for the higher-order orthogonal iteration (HOOI) algorithm applied to the quadruply-excited amplitudes.

```

generate starting values for  $V_{ai}^A$ ;
set  $\|t\|_0 = 0$  and conv. threshold  $\epsilon$ ;
for  $n = 1$  to maxit do
    set  $M_{ai,bj} = 0$ ;
    for  $D = 1$  to  $N_{\text{qua}}$  do
        | compute  $t_{ai,BCD}$  with fixed  $D$  index;
        |  $t_{ai,BCD} t_{bj,BCD} \rightarrow M_{ai,bj}$ , accumulate;
    end
    compute  $\|t\|_n$ , see Eq. (28);
    if  $\|t\|_n - \|t\|_{n-1} < \epsilon$  then exit;
    set  $\|t\|_{n-1} = \|t\|_n$ ;
    diagonalize  $M_{ai,bj}$ ;
    find  $N_{\text{qua}}$  eigenvectors with the largest
    eigenvalues and place them in updated  $V_{ai}^A$ ;
end

```

According to the above discussion, the critical part of the HOOI algorithm is the calculation of partly projected quadruply-excited amplitudes, Eq. (25). Without invoking any approximations, the computational cost of this step is proportional to N^9 , even under the assumption that N_{qua} scales linearly with the system size. This offers no practical advantages over the available conventional algorithms for calculation of the quadruples corrections. The main reason behind this steep scaling is the presence of the four-particle energy denominator in Eq. (5) which has to be eliminated in order to enable any scaling reduction. To this end, we employ the discrete Laplace transformation (LT) technique

$$(\epsilon_{ijkl}^{abcd})^{-1} = \sum_g^{N_g} w_g e^{-t_g(\epsilon_i^a + \epsilon_j^b + \epsilon_k^c + \epsilon_l^d)}, \quad (29)$$

where t_g and w_g are the quadrature nodes and weights, respectively, N_g is the size of the quadrature, and $\epsilon_i^a = \epsilon_i - \epsilon_a$. For the two-particle energy denominator this method was first proposed by Almlöf⁶⁴ in the context of the MP2 theory, but since then it has been successfully used in combination with other electronic structure methods.^{65–70} In this work we employ the min-max quadrature proposed by Takatsuka and collaborators^{71–73} for the choice of t_g and w_g . The number of quadrature points in Eq. (29) is independent of the system size, that is $N_g \propto N^0$. To the best of our knowledge, this is the first application of the LT technique to the four-particle energy denominator in the coupled-cluster theory.

The quadruply-excited amplitudes defined by Eq. (5) are given by the following explicit expression

$$t_{ijkl}^{abcd} = (\epsilon_{ijkl}^{abcd})^{-1} \Gamma_{ijkl}^{abcd}, \quad (30)$$

where

$$\begin{aligned} \Gamma_{ijkl}^{abcd} = \frac{1}{2} P_{ijkl}^{abcd} & \left[(ai|be) t_{jkl}^{ecd} - (ai|mj) t_{mkl}^{bcd} + (nj|mi) t_{mk}^{ac} t_{nl}^{bd} \right. \\ & \left. - 2(ai|me) t_{kj}^{eb} t_{ml}^{cd} - 2(be|mi) t_{kj}^{ce} t_{ml}^{ad} + (cf|ae) t_{ij}^{eb} t_{kl}^{fd} \right]. \end{aligned} \quad (31)$$

The permutation operator P_{ijkl}^{abcd} in the above formula reads

$$P_{ijkl}^{abcd} = (1 + P_{ai,bj}) (1 + P_{ai,ck} + P_{bj,ck}) (1 + P_{ai,dl} + P_{bj,dl} + P_{ck,dl}), \quad (32)$$

and $P_{ai,bj}$ denotes the basic transposition operator that exchanges pairs of indices $i \leftrightarrow j$ and $a \leftrightarrow b$ simultaneously. By employing the LT technique, we rewrite Eq. (25) in the form

$$t_{ai,BCD} = \sum_g^{N_g} w_g e^{-t_g \epsilon_i^a} \Gamma_{ijkl}^{abcd} \hat{V}_{bj}^{Bg} \hat{V}_{ck}^{Cg} \hat{V}_{dl}^{Dg} = \sum_g^{N_g} w_g e^{-t_g \epsilon_i^a} \gamma_{ai,BCD}^g, \quad (33)$$

with $\hat{V}_{bj}^{Bg} = V_{bj}^B e^{-t_g \epsilon_j^b}$ and $\gamma_{ai,BCD}^g = \Gamma_{ijkl}^{abcd} \hat{V}_{bj}^{Bg} \hat{V}_{ck}^{Cg} \hat{V}_{dl}^{Dg}$. Within this formulation of the

problem, the overall scaling of assembling the quantity $t_{ai,BCD}$ can be reduced to the level of N^6 . To illustrate this, let us consider a term $(bj|ae) t_{ikl}^{ecd}$ obtained by permutation of indices from the first term in Eq. (31). In the conventional implementation, this term scales as $O^4 V^5$. However, a contribution of this term to the quantity $\gamma_{ai,BCD}^g$ required in Eq. (33) can be factorized as

$$\begin{aligned} \gamma_{ai,BCD}^g &\longleftarrow (bj|ae) t_{ikl}^{ecd} \hat{V}_{bj}^{Bg} \hat{V}_{ck}^{Cg} \hat{V}_{dl}^{Dg} = \\ &\left((B_{ae}^Q U_{ei}^X) (B_{bj}^Q \hat{V}_{bj}^{Bg}) \right) \left[\left(t_{XYZ} (U_{ck}^Y \hat{V}_{ck}^{Cg}) \right) (U_{dl}^Z \hat{V}_{dl}^{Dg}) \right], \end{aligned} \quad (34)$$

where we have exploited the density-fitting factorization of the electron repulsion integrals, see Eq. (3), and Tucker factorization of the triply-excited amplitudes tensor given by Eq. (2). The parentheses included in the above formula indicate the order of operations and should be read starting from the innermost bracket. By following the optimal order of contractions one can show that the most costly step scales as $N_g OVN_{\text{SVD}}N_{\text{qua}}^3 \propto N^6$. Similar factorizations are possible for the remaining terms appearing in Eq. (31) and in every case the scaling is proportional to N^6 , albeit with different prefactors. However, the number of terms in Eq. (31) that have to be factorized is large – 144 in total if all permutations resulting from the action of the P_{ijkl}^{abcd} are taken into account. Therefore, explicit factorized formulas for the quantity $\gamma_{ai,BCD}^g$ are given in Supporting Information, along with a detailed discussion of possible simplifications.

Let us point out that the cost of the complete HOOI procedure is still asymptotically proportional to N^7 due to the need to assemble the $M_{ai,bj}$ matrix, see Eq. (27). However, this step can be formulated as a single DGEMM matrix-matrix multiplication and hence possesses a relatively small prefactor. Therefore, the calculation of the quantity $\gamma_{ai,BCD}^g$, in spite of the N^6 scaling, constitutes the majority of the total cost of the HOOI procedure for systems that can currently be studied.

The presentation given in this section has been focused on the t_{ijkl}^{abcd} amplitudes. However, the Algorithm 1 is straightforwardly adapted for an analogous decomposition of the

remaining quantities, namely the l_{ijk}^{abc} and l_{ijkl}^{abcd} amplitudes that parametrize the L_3 and L_4 operators. This is particularly seamless in the latter case as the only change required is the modification of Eq. (25) without affecting any other steps of Algorithm 1. Efficient evaluation of the modified expression is discussed in Supporting Information and it is shown that the scaling of this step is N^5 , i.e. lower than in the case of the t_{ijkl}^{abcd} amplitudes. Somewhat more advanced modifications of the HOOI procedure are required for the l_{ijk}^{abc} amplitudes. First, instead of Eq. (25) one calculates $l_{ai,Y'Z'} = l_{ijk}^{abc} U_{bj}^{Y'} U_{ck}^{Z'}$, and the matrix $M_{ai,bj}$ required in Algorithm 1 is obtained as $M_{ai,bj} = l_{ai,Y'Z'} l_{bj,Y'Z'}$, cf. Eq. (27). The remaining steps of the HOOI procedure are not affected. In Supporting Information we provide a factorized expression that enables to compute the intermediate quantity $l_{ai,Y'Z'}$ with N^6 cost, meaning that the decomposition of the l_{ijk}^{abc} amplitudes scales as N^6 overall.

To sum up the theoretical section of the paper, we point out that computation of the $\mathcal{L}_{(Q)}$ functional involves several steps, some of which have to be performed in a predefined order. For completeness, these steps are summarized in the Supporting Information, identifying the relevant key equations and presenting additional technical details. Importantly, by analyzing the working expressions we show that all components of the $\mathcal{L}_{(Q)}$ functional can be evaluated with a cost proportional to N^7 or less. A numerical confirmation of this finding is provided in the next section.

3 Numerical results and discussion

3.1 Computational details

Unless explicitly stated otherwise, in all calculations reported in this work employ the correlation-consistent cc-pVXZ basis set from Ref. 74. The corresponding density-fitting auxiliary basis sets cc-pVXZ-RIFIT were taken from the work of Weigend et al.⁷⁵ In some calculations, specified further in the text, a larger cc-pV5Z-RIFIT basis from Ref. 76 was employed to minimize the density-fitting error. Pure spherical representation ($5d$, $7f$, etc.)

of all Gaussian basis sets is adopted throughout. Density-fitting approximation is used in all correlated calculations unless written otherwise. However, the Hartree-Fock equations are solved using the exact two-electron integrals and hence the canonical HF orbitals are exact within the given one-electron basis. The frozen-core approximation is invoked in all computations reported in this work, unless explicitly stated otherwise. The $1s^2$ core orbitals of the first-row atoms (Li–Ne) are not correlated.

The reference CCSDT(Q) calculations and calculation of zero-point vibrational energies and harmonic frequencies were performed with the CFOUR program package.^{77,78} Some of the more demanding CCSD(T) calculations reported in this work, indicated below, were performed using NWChem program,⁷⁹ version 6.8. The calculations performed using the CFOUR and NWChem programs do not use the density-fitting approximations. All theoretical methods described in this work were implemented in a computer program written specifically for this purpose which is available from the author upon request. The TBLIS library⁸⁰ is used in the code for performing efficient tensor operations. It is worth mentioning that TBLIS natively supports shared-memory multiprocessing (using OpenMP application programming interface in our case) and hence most of the calculations reported in this work are performed in parallel, unless specified otherwise. Speed-ups by approximately a factor of 10 were observed in large-scale calculations on 12 (internode) threads. Beyond this point overheads related to, e.g. load balancing and synchronization, become significant and further increase of the number of computing threads leads to diminishing returns. A higher level of parallelization is possible using the MPI standard. This requires to divide the workload into independent task and, in the present context, it is natural to distribute the B_{pq}^Q three-center integrals by splitting the index Q among the computing nodes. However, this possibility has not been exploited in the present work. Lastly, the current implementation of the proposed theory does not utilize spatial symmetry of the molecules. Therefore, all calculations reported in this work are performed within C_1 symmetry group.

To avoid confusion, we briefly touch upon the naming conventions used in this section.

The abbreviation SVD-CCSDT designates the iterative rank-reduced CC method introduced in Ref. 14, and described briefly in Sec. 2.1, which is based on the Tucker compression of the triple excitation amplitudes, Eq. (2). The abbreviation SVD-CCSDT+ refers to a method introduced in Ref. 16. It consists of adding a non-iterative correction that accounts for triple excitations outside the subspace used in SVD-CCSDT calculations. In this way, the error with respect to the exact CCSDT method is reduced, even if the subspace of triple excitations used in Eq. (2) is small. Note that both SVD-CCSDT and SVD-CCSDT+ methods become functionally equivalent to the exact CCSDT for a sufficiently large value of the N_{SVD} parameter that controls the expansion length in Eq. (2).

3.2 Scaling demonstration

The efficiency of the proposed method hinges on the assumption that the parameter N_{qua} , which determines the size of the quadruple excitation subspace in Eq. (14), scales linearly with the system size, N . In other words, to retain a constant relative accuracy in the correlation energy as the system size grows, it is sufficient to set N_{qua} proportional to N . This conjecture is non-trivial because in the limit of the complete quadruple excitation subspace N_{qua} scales quadratically with the system size (more precisely, it is equal to the number of occupied times the number of virtual orbitals in the system).

In previous works, the property that dimension of the excitation subspace scales linearly with the system size has been demonstrated numerically for lower-dimensional (two- and three-) analogs of Eq. (14) using realistic model systems such as linear alkanes or water clusters for which reference CCSD/CCSDT results are available.^{12,14,17} Unfortunately, evaluation of the (Q) correction for systems comprising more than 4 – 5 non-hydrogen atoms is computationally costly, and hence reference results are not available for these model systems of sufficient size to reach definite conclusions about the behavior of N_{qua} . As a compromise, we adopt linear hydrogen chains as a model systems for the purposes of the scaling demonstration. The chain is composed of H_2 molecules (bond length 1.4 a.u.) with all hydrogen

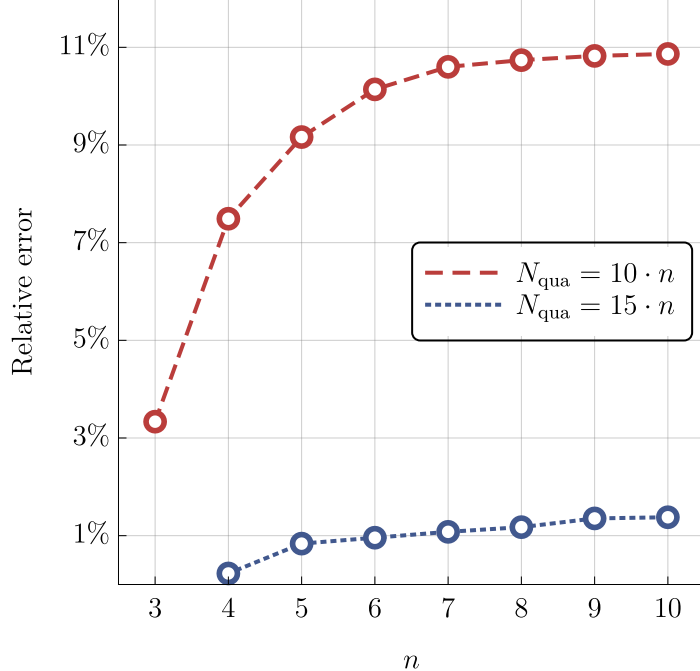


Figure 1: Percentage error in the (Q) correction obtained using the $\mathcal{L}_{(Q)}$ functional (cc-pVDZ basis set) for the $(H_2)_n$ system, $n = 3, \dots, 10$, with $N_{\text{qua}} = 10 \cdot n$ and $N_{\text{qua}} = 15 \cdot n$. The exact CCSDT(Q) results are used as a reference.

atoms placed co-linearly, hence the general formula $(H_2)_n$. The distance between centers of mass of two neighboring hydrogen molecules is equal 4.2 a.u. This system behaves as an insulator even in the limit of an infinite chain length, i.e. $n \rightarrow \infty$, which makes the single-reference CC approach valid.

We performed calculations of the quadruples corrections using the exact CCSDT(Q) method as implemented in CFOUR and the $\mathcal{L}_{(Q)}$ functional for the $(H_2)_n$ system, $n = 1, 2, \dots, 10$, within the cc-pVDZ basis set. We focus solely on the scaling of the N_{qua} parameter and hence employ the full space of triple excitations in the SVD-CCSDT calculations preceding the evaluation of the $\mathcal{L}_{(Q)}$ functional. In Fig. 1 we show relative errors in the calculated (Q) correction for a representative value of the quadruple excitation subspace size equal to $N_{\text{qua}} = 10 \cdot n$ and $N_{\text{qua}} = 15 \cdot n$, where n is the chain length. As the value of n increases, the relative error quickly reaches the asymptotic values of approximately 11% and 1%, respectively. In the region beyond $n \approx 7$ the error is essentially constant with only

minor fluctuations of the order of 0.1% or less. This confirms that in order to maintain a constant relative accuracy in the (Q) correction it is sufficient to make N_{qua} proportional to the system size.

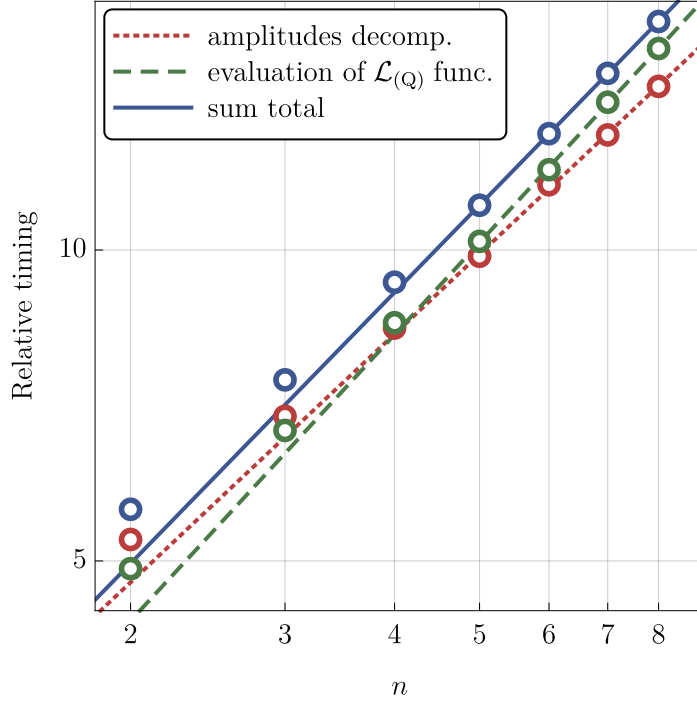


Figure 2: Relative timings of two major computational steps of the proposed formalism (cc-pVDZ basis set) for linear alkanes (C_nH_{2n+2}) as a function of the chain length, n . Logarithmic scale is used on both axes.

Another numerical demonstration necessary to confirm the theoretical findings of the present work is related to the computational cost of evaluating the $\mathcal{L}_{(Q)}$ functional. The analysis of the working equations of the proposed method given in Secs. 2.2-2.4 (and in Supporting Information) led to the conclusion that all terms in the $\mathcal{L}_{(Q)}$ functional can be computed with the cost proportional to N^7 in the rate-determining steps. Regarding the decomposition of the T_4 and L_4 amplitudes, they formally share the same N^7 asymptotic cost, but involve only one N^7 step that has a small prefactor. Therefore, we expect that this component of the method would possess, in practice, a cost proportional to N^6 . Finally, the decomposition of the L_3 amplitudes was found to scale as N^6 .

To confirm the aforementioned findings numerically, we perform calculations for model

systems that can be systematically increased in size. In contrast with the calculations considered at the beginning of this section, the reference CCSDT(Q) calculations are not involved here and hence it is feasible to study a more chemically appealing model system of linear alkanes, C_nH_{2n+2} . Molecular geometries were taken from Ref. 14. As an illustrative example, we set $N_{\text{SVD}} = N_{\text{MO}}$ and $N_{\text{qua}} = N_{\text{MO}}$, where N_{MO} is the number of orbitals in the system, so that both parameters increase linearly with the chain length. The core $1s^2$ orbitals of the carbon atoms are not correlated. In Fig. 2 we report total timings of the calculations, as well as timings for two major parts, namely (i) evaluation of the $\mathcal{L}_{(Q)}$ functional, and (ii) decomposition of the T_4 , L_3 , and L_4 amplitudes. For clarity, the timings are given in relation to the calculations for methane. To confirm that the results given in Fig. 2 match the theoretical predictions, we fitted the timings with the functional form $a \cdot n^b$ (a linear function on a logarithmic scale) for $n = 3 - 8$. We obtained the exponents $b = 6.64$ and $b = 5.76$ for the parts (i) and (ii), respectively. The empirically found values of the exponents are in both cases somewhat smaller than predicted theoretically (7 and 6). This can be explained by the fact that both parts of the calculations involve also many lower-scaling steps such as computation of intermediate quantities, etc. While the cost of such steps is asymptotically marginal, they still contribute non-negligibly to the total workload for systems that can be studied at present.

3.3 Calibration of the method

In this section we study errors of the proposed formalism in reproduction of the absolute (Q) correction. For this purpose we selected a set of 16 small molecules comprising 2 – 5 first row atoms. Within the cc-pVTZ basis set employed in the calculations, the largest molecule is described by 118 atomic orbitals and hence the conventional CCSDT(Q) calculations are feasible with a reasonable computational cost. Therefore, the values of the exact (Q) correction are available for each molecule and shall be used as reference in the present section. The list of molecular systems used in the benchmark calculations and their structures in

Cartesian coordinates are provided in the Supporting Information. To assure that the error resulting from the density-fitting approximation does not contaminate the final conclusions of this section, a large cc-pV5Z-RI auxiliary basis set is used. We verified that this leads to errors of no larger than a few μH in the correlation energies which is entirely negligible in the present context.

An important aspect of the analysis provided below relates to the determination of the recommended values of the quantities N_{SVD} and N_{qua} that serve as parameters in the rank-reduced formalism in the present work. The former parameter determines the size of the triple excitation subspaces used in T_3 and L_3 operators, see Eq. (2), while the latter serves the same purpose in the case of the quadruple excitation subspaces in T_4 and L_4 . As the cost of the calculations increases steeply with increasing N_{SVD} and N_{qua} , it is necessary to recommend a way of determining these parameters for a given system such that a sufficient level of accuracy is attained while the computational cost is simultaneously minimized. Since both N_{SVD} and N_{qua} increase linearly with the system size, it is convenient to tie them to some quantity that shares the same property, but is known upfront for a given system. In this way, the parameters can be easily transferred between molecules of different size. Similarly to previous works, we express the parameters N_{SVD} and N_{qua} as a fraction times the total number of active molecular orbitals in the system, N_{MO} (frozen-core orbitals and possibly frozen virtual orbitals are excluded). In other words, these parameters are given by $N_{\text{SVD}} = x \cdot N_{\text{MO}}$ and $N_{\text{qua}} = y \cdot N_{\text{MO}}$, where x, y are asymptotically independent of the system size. Note that both x and y may be larger than the unity. It has been shown in Ref. 14 that in reproduction of the CCSDT correlation energy $N_{\text{SVD}} \approx N_{\text{MO}}$ is sufficient in usual applications. However, it cannot be guaranteed *a priori* that a similar size of the triple excitation subspace is adequate in determination of the (Q) corrections.

Since the molecules included in the test set vary considerably in size, it is necessary to use a size-intensive error measure to compare the results. First, we consider the mean absolute percentage error (MAPE) averaged over all molecules. In Fig. 3 we plot MAPE as a

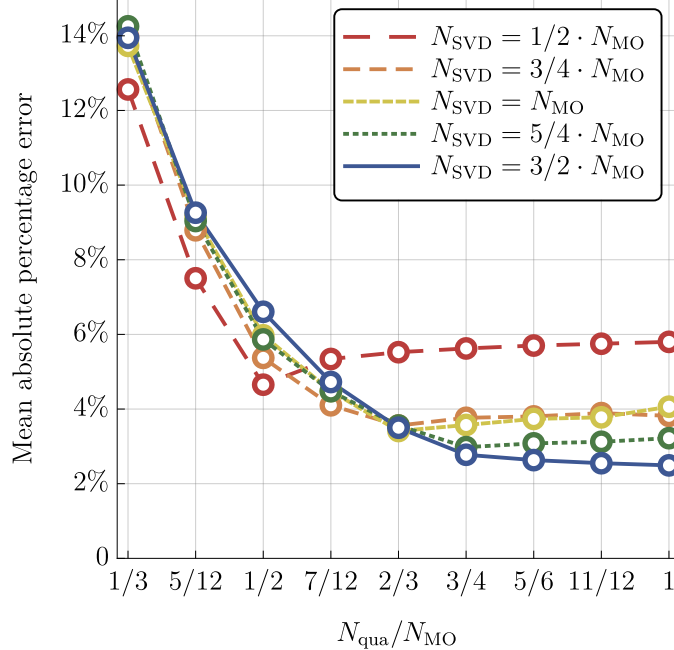


Figure 3: Mean absolute percentage error in the (Q) correction obtained using the $\mathcal{L}_{(Q)}$ functional (cc-pVTZ basis set) as a function of N_{qua} for several representative values of the N_{SVD} parameter, see the legend. The exact CCSDT(Q) results are used as a reference. The symbol N_{MO} denotes the total number of orbitals in a given system.

function of N_{qua} varied from $\frac{1}{3}N_{\text{MO}}$ to N_{MO} for several representative values of N_{SVD} , namely $N_{\text{SVD}} = x \cdot N_{\text{MO}}$ with $x = \frac{1}{2}, \frac{3}{4}, 1, \frac{5}{4}, \frac{3}{2}$. Overall, for each value of N_{SVD} individually, we observe a similar trend in error decay as N_{qua} is increased. Initially, the error vanishes rapidly, which is followed by a plateau region where the error stabilizes, see Fig. 3. Beyond this point, further increase of the N_{qua} parameters leads to no appreciable accuracy improvements, and in some cases the error even increases by a tiny amount. Clearly, in this region the accuracy is limited by the error of the triply-, and not quadruply-excited, amplitudes. This is further confirmed by the observation that the error in the plateau region depends significantly on N_{SVD} . For $N_{\text{SVD}} = \frac{1}{2}N_{\text{MO}}$ the error stabilizes at the level of around 6%; this decreases to around 4% for $N_{\text{SVD}} = N_{\text{MO}}$, and to slightly above 2% for $N_{\text{SVD}} = \frac{3}{2}N_{\text{MO}}$.

To recommend values of the parameters N_{SVD} and N_{qua} that shall be used in future calculations, we require that the MAPE in Fig. 3 should be at the order of a few percent, according to the discussion in the Introduction. The smallest triple excitation subspace

that systematically delivers the accuracy better than 5% corresponds to $N_{\text{SVD}} = \frac{3}{4}N_{\text{MO}}$ or $N_{\text{SVD}} = N_{\text{MO}}$. Smaller values of N_{SVD} are not recommended, unless supported by some reference calculations that confirm their reliability or if larger errors are acceptable. Further increase, to about $N_{\text{SVD}} = \frac{3}{2}N_{\text{MO}}$, of the parameter N_{SVD} is necessary to reach accuracy levels of 2% or so. Regarding the value of the second parameter, it is desirable to set N_{qua} to a value that (for a given N_{SVD}) corresponds as closely as possible to the onset of the plateau region. In this way the computational cost of the procedure is minimized without compromising the accuracy. A conservative choice is to set $N_{\text{qua}} = \frac{2}{3}N_{\text{SVD}}$, such that for each $N_{\text{SVD}} \geq N_{\text{MO}}$ the value of N_{qua} lies well-within the plateau region. We recommend this setup in future calculations. This approach has one additional advantage: the values of N_{SVD} and N_{qua} do not have to be varied independently. Instead, they are increased simultaneously which makes the results easier to analyze and represent.

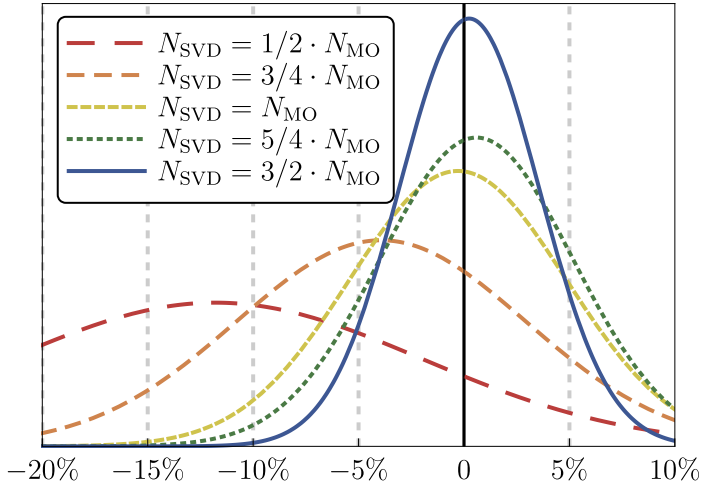


Figure 4: Distribution of relative errors (in percent) in the (Q) correction obtained using the $\mathcal{L}_{(Q)}$ functional (cc-pVTZ basis set) for several representative values of the N_{SVD} parameter, see the legend. For each value of N_{SVD} , the parameter N_{qua} is set to $\frac{2}{3}N_{\text{SVD}}$. The exact CCSDT(Q) results are used as a reference. The symbol N_{MO} denotes the total number of orbitals in a given system.

Thus far we have concentrated on MAPE as a measure of error of the proposed formalism. While this error measure is particularly important from the practical point of view, it provides little information about the error distribution and its characteristics. To fill this gap we

consider signed percentage error defined as

$$\Delta^{(i)} = 100\% \cdot \frac{\mathcal{L}_{(Q)}^{(i)} - E_{(Q)}^{(i)}}{E_{(Q)}^{(i)}}, \quad (35)$$

where the index i enumerates the molecules in the test set, and $E_{(Q)}^{(i)}$ is the reference (exact) value of the (Q) correction for the i -th molecule. For the purposes of statistical analysis we calculate the mean error, $\bar{\Delta}$, and its standard deviation, Δ_{std} using the well-known formulas. For all cases considered here we found that the error distribution is normal to a good degree of approximation. Therefore, for clarity we represent the error measures $\bar{\Delta}$ and Δ_{std} graphically in Fig. 4 in terms of normalized Gaussian distributions. As illustrative examples we consider $N_{\text{SVD}} = x \cdot N_{\text{MO}}$ with $x = \frac{1}{2}, \frac{3}{4}, 1, \frac{5}{4}, \frac{3}{2}$, and in each case we set $N_{\text{qua}} = \frac{2}{3}N_{\text{SVD}}$ according to the discussion above. As seen in Fig. 4, the accuracy obtained with $N_{\text{SVD}} = \frac{1}{2} \cdot N_{\text{MO}}$ and $N_{\text{SVD}} = \frac{3}{4} \cdot N_{\text{MO}}$ is not satisfactory. Although in the latter case the mean error is acceptable ($\bar{\Delta} < 5\%$), the corresponding standard deviation is still large ($\Delta_{\text{std}} \approx 6.8\%$) and hence the error distribution is rather broad. The results are improved considerably for $N_{\text{SVD}} = N_{\text{MO}}$ and $N_{\text{SVD}} = \frac{5}{4} \cdot N_{\text{MO}}$, where the mean error decreases to $\bar{\Delta} \approx -0.29\%$ and $\bar{\Delta} \approx 0.59\%$, respectively. This is accompanied by a significant reduction of the standard deviation. Finally, by increasing the value of the parameter N_{SVD} to $\frac{3}{2} \cdot N_{\text{MO}}$, the mean error is further reduced slightly ($\bar{\Delta} \approx 0.24\%$), similarly as the standard deviation ($\Delta_{\text{std}} \approx 3.3\%$).

Next, we consider errors of the proposed formalism in reproduction of relative energies. To this end, we prepared the following set of 10 chemical reactions:

1. $\text{F}_2 + \text{H}_2 \rightarrow 2\text{HF}$,
2. $\text{H}_2\text{O}_2 + \text{H}_2 \rightarrow 2\text{H}_2\text{O}$,
3. $\text{CO} + \text{H}_2 \rightarrow \text{H}_2\text{CO}$,
4. $\text{CO} + 3\text{H}_2 \rightarrow \text{CH}_4 + \text{H}_2\text{O}$,
5. $\text{N}_2 + 3\text{H}_2 \rightarrow 2\text{NH}_3$,
6. $\text{HCOOH} \rightarrow \text{CO}_2 + \text{H}_2$,
7. $\text{CO} + \text{H}_2\text{O} \rightarrow \text{CO}_2 + \text{H}_2$,

8. $\text{HCN} + \text{H}_2\text{O} \rightarrow \text{CO} + \text{NH}_3$,
9. $\text{HCN} + \text{NH}_3 \rightarrow \text{N}_2 + \text{CH}_4$,
10. $\text{H}_2\text{CO} + \text{H}_2\text{O}_2 \rightarrow \text{HCOOH} + \text{H}_2\text{O}$.

Contribution of the (Q) correction to each reaction energy has been computed with three different schemes (all within the cc-pVTZ orbital basis set). First, the exact CCSDT(Q) calculations that employ neither decomposition of the excitation amplitudes nor density-fitting approximation are used as a benchmark. The second and third scheme involves the quadratic (Q) functional with the recommended settings, namely $N_{\text{qua}} = \frac{2}{3}N_{\text{SVD}}$, and for several representative N_{SVD} . In the second scheme we use a large cc-pV5Z-RI auxiliary basis set for density-fitting approximation and hence the DF errors are marginal. In the third scheme the same settings are used, except that the standard cc-pVTZ-RI auxiliary basis set (matched to the used orbital cc-pVTZ) is employed. This enables us to study the impact of the density-fitting approximation on the quality of the results and establish whether the conventional auxiliary basis sets available in the literature are sufficient for the present purposes.

In Tables 2 and 3 we report results of the calculations with the large and standard density-fitting basis sets, respectively. As expected, for $N_{\text{SVD}} = \frac{1}{2}N_{\text{MO}}$ and $N_{\text{SVD}} = \frac{3}{4}N_{\text{MO}}$ average errors are substantial from the present point of view. However, as the size of the excitation subspace is increased to $N_{\text{SVD}} = N_{\text{MO}}$, the average absolute errors decrease to about 0.1 kJ/mol. This confirms that the recommended settings perform well in determination of the relative energies. Additionally, by comparing the results presented in Tables 2 and 3 one finds that the density-fitting approximation has a tiny impact on the quality of the results. The average DF errors are of the order of 0.01 kJ/mol and even the largest error found for the test set is well below 0.1 kJ/mol. Therefore, we conclude that the standard auxiliary basis sets (optimized for a given orbital basis) are sufficient for accurate determination of the (Q) correction.

It must be pointed out that with the parameters N_{SVD} and N_{qua} set as fixed multiples

Table 2: Contribution of the (Q) correction to the reaction energies calculated using the exact CCSDT(Q) method and using the quadratic (Q) functional as a function of N_{SVD} (with fixed $N_{\text{qua}} = \frac{2}{3}N_{\text{SVD}}$). The mean absolute error (MAE) and the standard deviation of the error (STD) are given in the last two rows. The cc-pVTZ orbital basis set is used together with a large cc-pV5Z-RI auxiliary basis set to eliminate the error due to the density-fitting approximation. All values are given in kJ/mol.

reaction	exact	$N_{\text{SVD}}^{\text{a}}$				
		$\frac{1}{2}N_{\text{MO}}$	$\frac{3}{4}N_{\text{MO}}$	N_{MO}	$\frac{4}{3}N_{\text{MO}}$	$\frac{3}{2}N_{\text{MO}}$
1	2.88	-0.12	-0.10	-0.12	-0.08	-0.06
2	1.52	-0.14	-0.20	-0.18	-0.10	-0.07
3	0.29	-0.12	0.02	0.06	0.02	0.02
4	1.61	-0.26	-0.10	0.04	0.01	0.01
5	3.15	-0.17	-0.06	0.12	0.13	0.10
6	-1.06	0.36	0.01	-0.17	-0.13	-0.05
7	-1.33	0.50	0.29	0.12	0.03	0.01
8	1.63	0.34	0.28	0.09	0.20	0.08
9	0.08	0.25	0.25	0.00	0.08	0.03
10	1.06	0.12	0.06	0.05	0.04	0.02
MAE	—	0.24	0.14	0.10	0.08	0.07
STD	—	0.27	0.17	0.12	0.10	0.07

^a Errors (for a given N_{SVD}) with respect to the exact result.

of some system-dependent quantity, the proposed method is not guaranteed to be size-consistent. This is true even one selects a multiple of a quantity that scales linearly with the system size, such as N_{MO} suggested in the previous paragraphs. While the results presented in this work, e.g. for the reaction energies, show that the size-inconsistency error is tiny, this can still become problematic in applications, e.g. to weakly-interacting systems, where proper cancellation of non-physical size-inconsistent contributions is important. One may argue from a pragmatic standpoint that if significant size-inconsistency errors are encountered, the simplest remedy is to increase the constant factor that relates N_{SVD} and N_{qua} to N_{MO} .

Table 3: The same data as in Table 2 but obtained using the standard cc-pVTZ-RI auxiliary basis set for the density-fitting approximation.

reaction	exact	$N_{\text{SVD}}^{\text{a}}$				
		$\frac{1}{2}N_{\text{MO}}$	$\frac{3}{4}N_{\text{MO}}$	N_{MO}	$\frac{4}{3}N_{\text{MO}}$	$\frac{3}{2}N_{\text{MO}}$
1	2.88	-0.16	-0.09	-0.06	-0.12	-0.06
2	1.52	-0.14	-0.29	-0.18	-0.11	-0.07
3	0.29	-0.11	0.02	0.08	0.03	0.03
4	1.61	-0.25	-0.14	0.05	0.01	0.09
5	3.15	-0.18	-0.08	0.13	0.13	0.10
6	-1.06	0.24	-0.17	-0.17	-0.12	-0.05
7	-1.33	0.39	-0.06	0.14	0.04	0.03
8	1.63	0.31	0.29	0.07	0.20	0.08
9	0.08	0.25	0.22	0.00	0.07	0.03
10	1.06	0.12	-0.20	0.04	0.03	0.02
MAE	—	0.21	0.16	0.09	0.08	0.07
STD	—	0.24	0.18	0.11	0.11	0.07

^a Errors (for a given N_{SVD}) with respect to the exact result.

As the rank-reduced formalism is built upon CC methods which are rigorously size-extensive, this approach is, in principle, always able to decrease these errors to acceptable levels. However, this line of reasoning is not fully satisfactory as it may lead to a significant increase of the computational costs. A more suitable approach would be to determine the size of the excitation subspace adaptively for a given molecule based on some numerical threshold that is transferable between systems. However, this problem is non-trivial as the higher-order orthogonal iteration algorithm applied to higher-order amplitudes does not provide a natural numerical parameter that can be used for the truncation, in contrast to, e.g. the diagonalization approach adopted in Ref. 12 for the doubly-excited amplitudes. Our preliminary tests have shown that a simple threshold on, e.g. the eigenvalues of the $M_{ai,bj}$ matrix defined by Eq. (27) are not entirely satisfactory. Therefore, a more elaborate scheme is required which

employs, e.g. a threshold on the cumulative eigenvalues of the $M_{ai,bj}$ matrix. A complete analysis of this problem requires numerous benchmarks calculations analogous to the data presented in Ref. 81. This is beyond the scope of the present paper and requires a separate study which is currently in progress.

Finally, after establishing the computational protocol that shall be used in subsequent applications, we can assess the computational performance of the proposed theory in comparison with the conventional (Q) implementation. While we have shown in the previous section that the rank-reduced formalism is characterized by a lower scaling with the system size than the exact (Q) method (N^7 vs. N^9), it is not yet clear how this translates into computational advantages. In fact, due to the overhead related to determination of the excitation subspace (and other steps of the rank-reduced calculations), one expects that the prefactor of the conventional (Q) algorithm is lower and hence there is a break-even point beyond which our method is favored. In order to approximately locate this break-even point, we compared the timings of the calculations reported in this section with the conventional (Q) algorithm as implemented in the CFOUR program (to allow a fair comparison, the same machine was used for both calculations and serial program execution was requested). Depending on the cardinal number of the basis set, the proposed algorithm becomes beneficial for systems with more than 100 – 150 basis set functions. For example, for the formic acid molecule in the cc-pVTZ basis set (115 active orbitals), the rank-reduced calculations are three times faster than the conventional algorithm. In general, our tests revealed that the break-even point occurs faster for smaller basis sets. However, we also would like to point out that the current pilot implementation of the rank-reduced formalism can be improved by more extensive code optimization. While, in principle, the same is true for the conventional (Q) algorithm, implementations of the latter are much more mature.

3.4 Isomerization energy of *ortho*/*meta* benzyne

As the first application of the proposed theory we study the isomers of benzyne molecule (C_6H_4) in singlet spin state. We are interested in the isomerization energy between *ortho*- and *meta*-benzyne. Benzyne have attracted a significant interest in recent years, both from experimental^{82,83} and theoretical point of view,^{84–91} due to their unique electronic structure and chemical properties. In synthetic organic chemistry, *ortho*-benzyne is a crucial intermediate in several important types of reactions, see the recent review paper of Tadross and Stoltz⁹² for an in-depth discussion. Benzyne are also found⁹³ to be the key intermediate in formation of polycyclic aromatic hydrocarbons – carcinogenic and environmentally-harmful compounds. In particular, the *ortho*- and *meta*-benzyne isomerization has been proposed to constitute an important step of various fragmentation and decomposition reaction pathways.^{94–96} From the theoretical standpoint, benzyne are known to possess a singlet diradical character of the ground-state energy level and it has been shown that static correlation effects play an important role in description of these systems. Therefore, benzyne are frequently employed in benchmark studies of novel quantum chemistry methods where accurate and reliable reference data is valuable.

Throughout the present section we adopt the convention that the isomerization energy ΔE is defined as

$$\Delta E = E_{meta} - E_{ortho}. \quad (36)$$

It is known that in the ground electronic singlet state the *ortho* isomer is more stable and hence the total isomerization energy defined above is positive. However, individual contributions to the isomerization energy representing various physical contributions may be of an arbitrary sign. For clarity, positive contributions are understood to favor the *ortho* isomer, while negative contributions – the *meta* isomer.

Besides studying the performance of the rank-reduced formalism for the isomers of ben-

yne, our goal is to show how the proposed method can be incorporated in the so-called composite electronic structure schemes in order to increase their accuracy, computational performance or range of applicability. Several families of composite schemes were proposed in the literature, e.g. Gaussian- n (G- n) originally introduced by Pople *et al.*,^{97–100} Weizmann- n (W- n) model chemistry developed by Martin and collaborators,^{101–103} or HEATxyz protocol in its several variants.^{104–106} Nowadays, composite schemes are an important tool in, e.g. *ab initio* thermochemistry calculations or theoretical prediction of quantitative chemical kinetics. The main idea behind the composite schemes is to split, e.g. the total electronic energy of a molecule, into a sum of one (in some variants, two) major components supplemented by a series of smaller additive corrections. Depending on the desired level of accuracy, the number of corrections varies from just a few to a dozen or so in the most demanding situations. As the corrections are small in absolute terms compared to the major components, they can be calculated less accurately – usually employing a smaller basis set or with some additional approximations. Below we introduce a composite method that targets the accuracy comparable to the exact CCSDT(Q) theory, and employs the rank-reduced approach to the calculation of the (Q) correction and the SVD-CCSDT+ method for determination of the triple excitation contributions.

The molecular geometries of *ortho*- and *meta*-benzyne were taken from the paper of Karton *et al.*⁹⁰ where they were optimized using the frozen-core CCSD(T)/cc-pVQZ method. Our preliminary study has shown that these structures are well-converged with respect to the basis set size and the CC level. Therefore, all subsequent calculations of contributions to the isomerization energy were performed at fixed CCSD(T)/cc-pVQZ geometries, unless explicitly stated otherwise.

We begin by considering the Hartree-Fock contribution to the isomerization energy which was calculated using the cc-pV X Z basis sets with $X=D,T,Q,5$. As expected, it converges very fast to the basis set limit, with the value calculated using the cc-pVQZ basis set, 106.90 kJ/mol, differs from the result obtained within the cc-pV5Z basis set, 106.97 kJ/mol,

by just 0.07 kJ/mol. To further minimize the basis set incompleteness error we perform three-parameter extrapolation using the exponential formula

$$E_X = E_\infty + A e^{-BX}, \quad (37)$$

where E_∞ , A , B are fitted to reproduce the results obtained within the largest three basis sets. This leads to the final result 106.99 kJ/mol. Taking into account the rapid convergence of the results with the basis set size, it is reasonable to assume that the error of this quantity is no larger than 0.05 kJ/mol.

Next, we move on to the valence CCSD contribution using the same basis sets as for the Hartree-Fock method. One obtains -37.08 , -34.90 , -33.52 , -32.99 kJ/mol with the $X=D,T,Q,5$ basis sets, respectively. The convergence pattern to the basis set limit is systematic, but the residual basis set error is still relatively large. To eliminate a significant portion of this error we employ the two-parameter Riemann extrapolation formula proposed in Ref. 107:

$$E_\infty = E_X + X^4 \left[\frac{\pi^4}{90} - \sum_{n=1}^X n^{-4} \right] (E_X - E_{X-1}). \quad (38)$$

This stencil is used for extrapolation of all correlation energies in the remainder of the present work. The extrapolated CCSD contribution using the $X = Q(4), 5$ basis sets reads -32.32 ± 0.34 kJ/mol, where the error was conservatively estimated to be equal to the half of the difference between the extrapolated value and the result in largest basis set available. This approach was found to provide reliable and conservative error estimates for small molecular systems at the same level of theory.^{107,108}

The next important contribution to the isomerization energy is the effect of triple excitations, defined as the difference of the results obtained with the CCSDT and CCSD methods. Due to cost considerations, it is a common practice to split the triple excitations contribution into two parts, namely (i) the contribution of triple excitations captured by the CCSD(T)

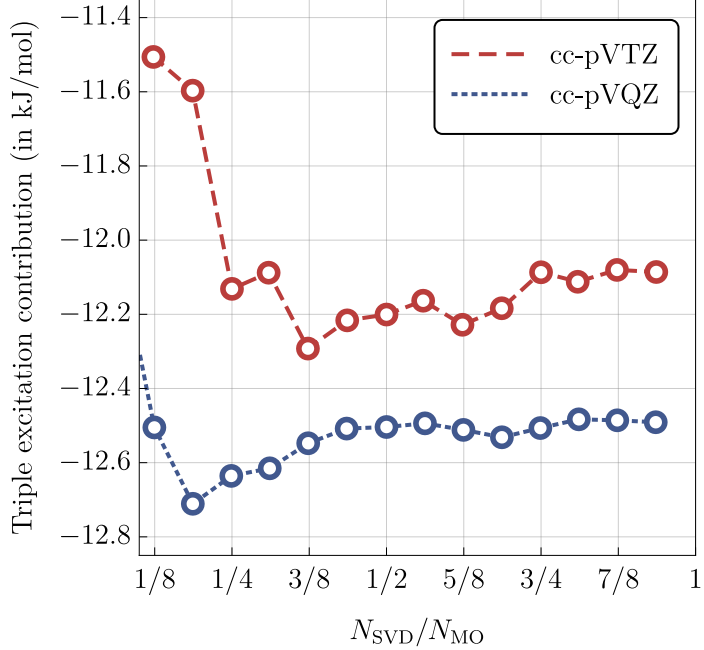


Figure 5: Triple excitation contribution to the isomerization energy of *ortho/meta* benzyne calculated using the SVD-CCSDT+ method (cc-pVTZ and cc-pVQZ basis sets) as a function of the N_{SVD} parameter. The symbol N_{MO} denotes the total number of orbitals in the system.

method and (ii) the remainder, i.e. the difference between the CCSD(T) and CCSDT results. This approach is justified by the fact that the first contribution is usually dominating and can be obtained with a larger basis set. However, in the present application we found this separation to be no longer beneficial if the SVD-CCSDT+ method is used for evaluation of the triple excitation effects. This is because the largest basis set we could use in both CCSD(T) and SVD-CCSDT+ calculations was cc-pVQZ. Despite significant effort, it was impossible to perform canonical (T)/cc-pV5Z calculation using the hardware and software available to us, either due to excessive computational time or memory/disk space limitations. Taking into consideration that SVD-CCSDT+ is more accurate, we use it directly to determine the effects of triple excitations, bypassing the (T) method. In Fig. 5 we show the convergence of the T_3 contribution (cc-pVTZ and cc-pVQZ basis sets) to the isomerization energy as a function of the N_{SVD} parameter. Similarly as in the previous sections, this parameter is expressed as $N_{\text{SVD}} = x \cdot N_{\text{MO}}$, where $x \in (0, 1]$. The results are remarkably stable with respect to the value of N_{SVD} ; for $x > \frac{1}{2}$ the results change by less than 0.1 kJ/mol with the smaller

basis and 0.05 kJ/mol with the larger basis. We take the results obtained with $x = 1$ as the limit which leads to 12.12 kJ/mol and 12.48 kJ/mol within cc-pVTZ and cc-pVQZ basis sets, respectively. We assign the uncertainty of 0.05 kJ/mol to both these values. To obtain the final value of the triple excitation contribution to the isomerization energy we perform two-point $X = T, Q$ complete basis set extrapolation, giving 12.80 ± 0.17 kJ/mol. Two sources of error contribute to the proposed uncertainty: the extrapolation error (0.16 kJ/mol) which was estimated in the same way as for the CCSD contribution, and the error due to the truncation of the triple excitation subspace (0.05 kJ/mol, see the discussion above related to the N_{SVD} parameter). Since both sources of error can be viewed as independent, the final error is calculated by summing their squares and taking the square root, according to the usual rules of error propagation.

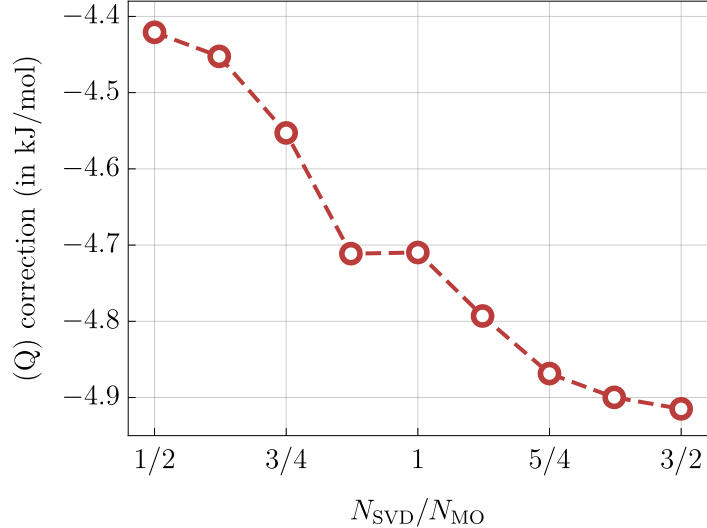


Figure 6: Quadruple excitation contribution to the isomerization energy of *ortho/meta*-benzyne calculated using the $\mathcal{L}_{(Q)}$ functional (cc-pVTZ basis set) as a function of the N_{SVD} parameter. For each value of N_{SVD} , the parameter N_{qua} is set to $\frac{2}{3}N_{\text{SVD}}$. The symbol N_{MO} denotes the total number of orbitals in the system.

Finally, we move on to the calculation of the (Q) correction which accounts for the quadruple excitation effects. For this purpose we adopt the quadratic functional formalism introduced in the present work combined with the cc-pVTZ basis set. We also follow the recommendations stated in the previous section and set $N_{\text{qua}} = \frac{2}{3}N_{\text{SVD}}$ in all calculations. In

Fig. 6 we present the (Q) contribution to the isomerization energy as a function of the N_{SVD} parameter. Beyond $N_{\text{SVD}} = N_{\text{MO}}$ changes in the (Q) correction are increasingly smaller. For example, upon increasing this parameter from $N_{\text{SVD}} = N_{\text{MO}}$ to $N_{\text{SVD}} = \frac{5}{4}N_{\text{MO}}$, the (Q) correction decreases by about 0.15 kJ/mol, while further increase to $N_{\text{SVD}} = \frac{3}{2}N_{\text{MO}}$ affects it only by ca. 0.04 kJ/mol. By following the trend seen in Fig. 6 one can expect that by further increase of the N_{SVD} parameter the (Q) correction will still decrease slightly. However, the changes are expected to be insignificant; even assuming the worst case scenario that the convergence of the (Q) correction is inversely proportional to N_{SVD} , the limit would be less than 0.1 kJ/mol away from the value obtained with $N_{\text{SVD}} = \frac{3}{2}N_{\text{MO}}$. As a result, we assume that the (Q) correction to the isomerization energy is equal to the value obtained for $N_{\text{SVD}} = \frac{3}{2}N_{\text{MO}}$, and assign conservative 0.1 kJ/mol error bars, giving -4.92 ± 0.10 kJ/mol. We neglect the basis set incompleteness error in calculation of the (Q) correction. The computations of the (Q) correction using the quadratic functional for benzyne molecule with $N_{\text{SVD}} = \frac{3}{2}N_{\text{MO}}$ and $\frac{2}{3}N_{\text{SVD}}$ (cc-pVTZ basis set) take about 2 days on 14 cores of AMD OpteronTM Processor 6174.

The last major contribution to the isomerization energy is the zero-point vibration energy (ZPVE). Unfortunately, computation of this quantity at the CC level is costly, especially if a large basis set is required. For this reason, we employ the B3LYP/cc-pVTZ method to determine the ZPVE correction to the isomerization energy. Within the harmonic oscillator approximation the ZPVE contribution equals to -4.34 kJ/mol. This value is further scaled by the recommended factor $f = 0.9764$ to take the anharmonic effects into account,¹⁰⁹ giving -4.24 kJ/mol. In order to estimate the error of this quantity, we note that in a recent work B3LYP/cc-pVTZ method^{110–113} was found to perform extremely well in comparison with CCSD(T) for molecules composed of first-row atoms.¹¹⁴ This is especially true for hydrocarbons, where the average deviation from CCSD(T) is just about 1%. Therefore, we conservatively assume that the error of the ZPVE contribution to the isomerization energy of *ortho/meta* benzyne does not exceed 5%, or 0.21 kJ/mol.

Table 4: Final error budget of the calculations of the isomerization energy of *ortho/meta* benzyne. All values are given in kJ/mol.

	contribution to ΔE
Hartree-Fock	106.99 ± 0.05
valence CCSD	-32.32 ± 0.34
valence T_3	-12.80 ± 0.17
valence (Q)	-4.92 ± 0.10
inner-shell correlation	2.00 ± 0.10
scalar relativity	-0.26 ± 0.04
DBOC	0.03 ± 0.10
ZPVE	-4.24 ± 0.21
total	54.52 ± 0.47
experiment	64.0 [83,115]
other theoretical	54.4^a [90]
	51.5^b [91]
	61.2^c [87]
	51.0^d [84]

^a W3.2lite(b) composite method

^b CAS(12,12)+PT2/CBS + ZPE_{CASSCF}

^c G2M(rcc,MP2) composite method¹¹⁶

^d CASPT2[g1]+aANO:C(5s4p2d)/H(3s2p) basis set

Finally, we consider several minor corrections that do not contribute significantly to the isomerization energy, but are nonetheless required in an accurate study. In the order of importance, we consider first the effect of the inner-shell $1s^2$ orbitals of carbon atoms on the isomerization energy. The inner shell correction was computed as a difference between all-electron and frozen-core CCSD(T) results obtained within the core-valence cc-pwCV X Z basis sets.¹¹⁷ In this way one obtains 0.64 kJ/mol, 1.60 kJ/mol and 1.81 kJ/mol for $X=D,T,Q$, respectively. Our final estimation, 2.00 ± 0.10 kJ/mol, is obtained by two-point extrapolation from the $X=T,Q$ pair, and the error is estimated in the same fashion as for the valence CCSD contribution.

The scalar relativistic effects were taken into account using DKH Hamiltonian^{118–120} as implemented in NWChem program.¹²¹ The relativistic correction was calculated at the all-electron CCSD(T)/cc-pwCVXZ level of theory, giving -0.23 , -0.19 , and -0.22 for $X=D,T,Q$, respectively. The final result, -0.26 ± 0.02 kJ/mol, was obtained using the same procedure as for the inner-shell correction. Lastly, the diagonal Born-Oppenheimer correction (DBOC, also known as the adiabatic correction in the literature) was calculated using the CCSD/cc-pVDZ method¹²² employing the CFOUR program. The result, equal to about 0.03 kJ/mol, signals that this effect has a negligible impact on the isomerization energy. While the size of the basis set used is small, and the obtained value is only a rough estimation, it is sufficient for the present purposes. However, we assign large error bars to this quantity, 0.03 ± 0.10 kJ/mol.

The results obtained in this section are summarized in Table 4 and compared with other data available in the literature. The comparison with the most recent experimental determination⁸³ reveals a substantial difference of about 10 kJ/mol. However, it has to be pointed out that the experimental value was obtained as a combination of atomization energies and the error of the final result is difficult to estimate. We find it likely that the theoretical value obtained in this work is considerably more accurate which is supported by other theoretical results found in the literature. They all tend to cluster around $\Delta E \approx 50 - 55$ kJ/mol which suggest that the experimental value should be revised down.

3.5 Cope rearrangement in bullvalene molecule

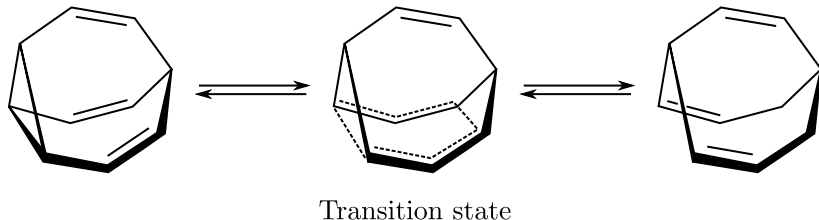


Figure 7: Chemical structures illustrating the Cope rearrangement in the bullvalene molecule.

The second system we study in this work in detail is the bullvalene molecule, $C_{10}H_{10}$. This molecule attracted considerable attention, because it is a prototypical fluxional molecule that possesses no permanent molecular structure, i.e. the nuclei are constantly in a concerted motion.¹²³ In bullvalene, this is enabled by the Cope rearrangement, exemplified in Fig. 7, that may occur between many equivalent configurations. The initial and final structure are degenerate, but are separated by a reaction barrier. While the bullvalene molecule has been synthesised a long time ago,^{124,125} and frequently studied both experimentally and theoretically since then, the height of the barrier is not established unambiguously. The most recent theoretical result of Karton *et al.*¹²⁶ differs from the experimental results (obtained by NMR techniques¹²⁷) by several kJ/mol. This discrepancy is much larger than the reported uncertainties of both calculations and measurements, and hence the theory and experimental data are not consistent at this point. In this section we carry an independent systematic theoretical study of the bullvalene Cope rearrangement barrier height and discuss the possible sources of this inconsistency. In particular, we include corrections due to triple and quadruple excitations calculated with the rank-reduced formalism. These corrections would be extremely costly to compute using the exact CCSDT(Q) method; in fact, we did not manage to accomplish CCSDT(Q) calculations even with the smallest cc-pVDZ basis.

The electronic contribution to the reaction barrier height is denoted by the symbol ΔE^\ddagger . For the purposes of direct comparison with the experimental data, we additionally need to calculate the Gibbs free energy barrier heights at the temperature $T = 298$ K. This quantity is denoted by ΔG_{298}^\ddagger and includes, besides ΔE^\ddagger , the zero-point vibrational energy (ZPVE) and enthalpic/entropic temperature corrections, as detailed below.

The molecular geometries of the bullvalene equilibrium structure and Cope rearrangement transition state were optimized at the B3LYP-D3/pc-2 level of theory^{128–131} using NWChem package. The obtained structures were verified to represent the equilibrium structure (real harmonic frequencies) and first-order transition state (one imaginary frequency). The Cartesian geometries of both structures are given in Supporting Information. The barrier height

ΔE^\ddagger is split into several components calculated at different levels of theory, and a composite scheme is used to assemble the best theoretical estimate. Because the bullvalene molecule is roughly twice as large as the systems considered in Sec. 3.4, the composite method applied here is less rigorous in nature. In particular, we do not assign uncertainties to individual contributions to the barrier height; instead, we attach a global error estimate only to the final result.

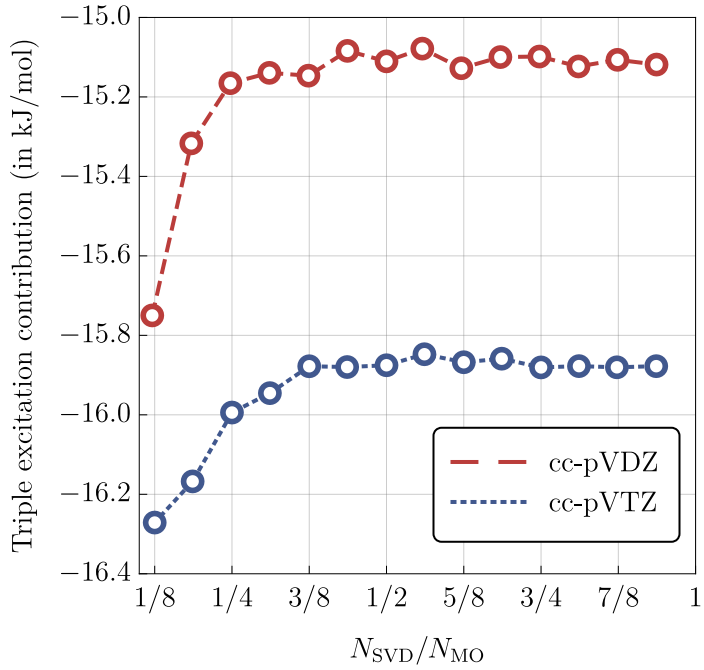


Figure 8: Triple excitation contribution to the Cope rearrangement barrier height (ΔE^\ddagger) in bullvalene molecule calculated using the SVD-CCSDT+ method (cc-pVDZ and cc-pVTZ basis sets) as a function of the N_{SVD} parameter. The symbol N_{MO} denotes the total number of orbitals in the system.

First, we consider the Hartree-Fock contribution to the barrier height which was calculated using the cc-pV X Z basis sets with $X=T,Q,5$. The exponential extrapolation (37) from these three basis sets leads to the result 108.97 kJ/mol. This differs by less than 0.1 kJ/mol from the result obtained within the cc-pV5Z basis, showing that the error of the Hartree-Fock component of ΔE^\ddagger is negligible. The second contribution to ΔE^\ddagger was calculated using the CCSD method, giving -29.20 , -28.39 , and -27.50 kJ/mol with cc-pV X Z, $X=D,T,Q$, basis sets, respectively. To further reduce the basis set incompleteness error we apply the two-point

extrapolation formula (38) resulting in the final CCSD contribution of -26.68 kJ/mol.

Next, we consider the contribution of triple excitations to the barrier height. It was computed using the SVD-CCSDT+ method within the cc-pVDZ and cc-pVTZ basis sets. Similarly as in the previous section, we do not split the effect of triple excitations into (T) and post-(T) components, because we did not manage to calculate the (T) correction within a larger (cc-pVQZ) basis set due to excessive time requirements. Note that the SVD-CCSDT+ calculations within the cc-pVTZ basis involve 50 correlated electrons and 440 atomic orbitals which vastly exceeds the capabilities of the available CCSDT implementations. In Fig. 8 we present triple excitation contribution to the barrier height as a function of the N_{SVD} parameter. The results saturate fast with respect to the value of N_{SVD} , and for $N_{\text{SVD}} = \frac{1}{2}N_{\text{MO}}$ they are essentially converged. Beyond this point minor fluctuations at the level of ca. 0.05 kJ/mol and 0.02 kJ/mol are observed, but this is completely negligible in comparison with other sources of error. Using the results obtained with $N_{\text{SVD}} = N_{\text{MO}}$, we obtain the contributions of triple excitations equal to -15.23 and -15.87 kJ/mol in the cc-pVDZ and cc-pVTZ basis sets, respectively. The final result, -16.26 kJ/mol, is obtained using two-point extrapolation formula, Eq. (38).

The quadruple excitation contribution to ΔE^\ddagger was calculated using the $\mathcal{L}_{(Q)}$ functional and the cc-pVDZ basis set. In Fig. 9 we present the (Q) correction as a function of the N_{SVD} parameter and with the recommended $N_{\text{qua}} = \frac{2}{3}N_{\text{SVD}}$. One can see that beyond $N_{\text{SVD}} = \frac{5}{4}N_{\text{MO}}$ the results are essentially stable with respect to this parameter. The variations are within $0.01 - 0.02$ kJ/mol and hence are negligible from the present point of view. Therefore, we take the value obtained with $N_{\text{SVD}} = \frac{3}{2}N_{\text{MO}}$, namely -2.29 kJ/mol, as the final contribution of quadruple excitations to ΔE^\ddagger . The computations of the (Q) correction using the quadratic functional for the bullvalene molecule with $N_{\text{SVD}} = \frac{5}{4}N_{\text{MO}}$ and $\frac{2}{3}N_{\text{SVD}}$ (cc-pVDZ basis set) take about 3 days on 14 cores of AMD OpteronTM Processor 6174.

The last contributions to ΔE^\ddagger are due to the inner-shell correlation and relativistic effects (scalar DKH Hamiltonian). They were both calculated using all-electron CCSD method

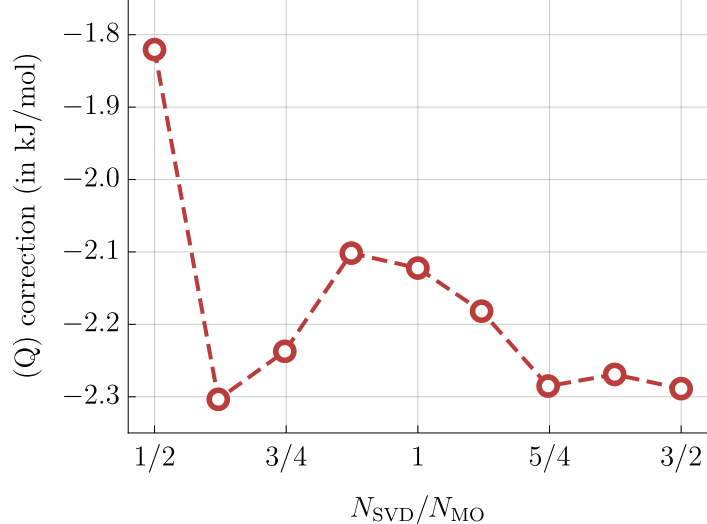


Figure 9: Quadruple excitation contribution to the Cope rearrangement barrier height (ΔE^\ddagger) in bullvalene molecule calculated using the $\mathcal{L}_{(Q)}$ functional (cc-pVDZ basis set) as a function of the N_{SVD} parameter. For each value of N_{SVD} , the parameter N_{qua} is set to $\frac{2}{3}N_{\text{SVD}}$. The symbol N_{MO} denotes the total number of orbitals in the system.

within cc-pwCVTZ basis set supplemented by (T) correction obtained within cc-pwCVDZ basis. No extrapolation towards the complete basis set was performed. This brings contributions to ΔE^\ddagger equal 1.33 and -0.21 kJ/mol due to the aforementioned two effects. We also estimated the DBOC component of ΔE^\ddagger (CCSD/cc-pVDZ level of theory) and found it to be negligible (< 0.1 kJ/mol) within the present accuracy standards.

Finally, ZPVE contribution to the barrier height, as well as thermal corrections, were calculated at the same level of theory as the geometry optimization (B3LYP-D3/pc-2). The raw value of ZPVE was additionally scaled by the empirical factor $f = 0.9678$, as recommended in Ref. 132, to take the anharmonic effects into account, giving -4.36 kJ/mol. Thermal corrections were calculated within the rigid rotor/harmonic oscillator approximations without frequencies scaling. The thermal enthalpic and entropic contributions to the Gibbs free energy barrier height for $T = 298$ K are -0.59 and 1.03 kJ/mol, respectively, and hence the total finite-temperature correction is just 0.44 kJ/mol.

The final results of the calculations of the Gibbs free energy barrier height for the Cope rearrangement in the bullvalene molecule are summarized in Table 5. The total ΔG_{298}^\ddagger

Table 5: Summary of the calculations of the Gibbs free energy barrier height for the Cope rearrangement in the bullvalene molecule. All values are given in kJ/mol.

contribution to ΔG_{298}^\ddagger	
Hartree-Fock	108.97
valence CCSD	−26.68
valence T_3	−16.26
valence (Q)	−2.29
inner-shell correlation	1.33
scalar relativity	−0.21
ZPVE	−4.36
thermal correction	0.44
total	60.94

determined by us equals to 60.94 kJ/mol. In order to roughly estimate the error of this result we note that there are two major sources of uncertainty: valence CCSD and ZPVE contributions. They can both lead to errors of the order of 0.5 kJ/mol. The remaining contributions to ΔG_{298}^\ddagger are expected to be accurate to within 0.1 – 0.2 kJ/mol. All in all, the value determined by us, $\Delta G_{298}^\ddagger = 60.94$ kJ/mol, has uncertainty of around 1 kJ/mol. This result is in reasonable agreement with the most recent theoretical result of Karton,¹²⁶ 62.21 kJ/mol, but in a disagreement with older calculations based on lower levels of theory which give results within 35 – 55 kJ/mol range.^{133–136} More strikingly, our result is in a disagreement with the experimental data of Moreno *et al.*¹²⁷ who obtained $\Delta G_{298}^\ddagger = 54.8 \pm 0.8$ kJ/mol from gas-phase NMR measurements. Such a large difference of about 6 kJ/mol is unlikely to be caused by an error in the theoretical protocol adopted by us. Therefore, we believe that the experimental data for this system should be reevaluated and a new measurement may help to resolve the persisting discrepancy between state-of-the-art theory and experimental results.

4 Conclusions and future work

In this work we have extended the rank-reduced coupled-cluster formalism to the calculation of non-iterative energy corrections due to quadruple excitations. The focus of the present work has been concentrated on the CCSDT(Q) method, which has become *de facto* standard in high-accuracy *ab initio* quantum chemistry, and can be viewed as the “platinum standard” of the field. The proposed formalism consist of two major novel components. The first is the application of the Tucker format to compress the quadruple excitation amplitudes and eliminate the full rank t_{ijkl}^{abcd} tensor entirely from the computational procedure. The second is the introduction of a modified functional for evaluation of the (Q) correction. This functional is rigorously equivalent to the standard (Q) formalism when the exact CC amplitudes are used. However, due to the fact that the new functional is stationary with respect to the amplitudes, it is less susceptible to errors resulting from the aforementioned compression. We show, both theoretically and numerically, that the computational cost of the proposed method scales as the seventh power of the system size. Using reference results for a set of small molecules, the method is calibrated to deliver accuracy of a few percent in relative energies. To illustrate the potential of the theory we calculate the isomerization energy of *ortho/meta* benzene (C_6H_4) and the barrier height for the Cope rearrangement in bullvalene ($C_{10}H_{10}$). In both cases we show that the proposed formalism considerably increases the range of applicability of the CC theory with non-iterative energy corrections due to quadruple excitations.

The present work is a starting point for a rank-reduced treatment of other quantum chemistry methods involving quadruple excitations. Indeed, the quadruple excitation subspace obtained by the HOOI procedure, Sec. 2.5, can be used also in more advanced (both iterative and non-iterative) CC models involving the T_4 operator. This includes even the complete CCSDTQ method. In fact, our preliminary study showed that the N^7 scaling can be achieved at the CCSDTQ level if both the triple and quadruple excitation amplitudes are compressed using the Tucker format. However, to exploit this advantage an efficient imple-

mentation is required to minimize the prefactor, and the accuracy of the resulting method must be thoroughly tested and calibrated.

Another important extension is generalization of the rank-reduced coupled-cluster formalism to the open-shell situations. This direction is especially important for applications in *ab initio* thermochemistry, where calculation of atomization energies is an important problem. A straightforward way to handle the open-shell systems is offered by the spin-unrestricted coupled-cluster theory, but this approach leads to the spin-contamination of the electronic wavefunction, as is well-documented in the literature.^{137–139} While the issue of spin-contamination may not be severe in many applications, a more pressing problem is the need to handle numerous spin cases of the triply- and, especially, quadruply-excited configurations. In the spin-unrestricted formalism each spin case has to be decomposed separately, leading to a significant increase in the computational costs. As a result, a more robust and advanced^{140–146} approach to the spin-adaptation in open-shell systems may be required which will be considered in future works.

Acknowledgement

I would like to thank Dr. A. Tucholska for fruitful discussions, and for reading and commenting on the manuscript. The author is grateful to Dr. D. Matthews for his help in effective usage of the TBLIS library. This work was supported by the National Science Center, Poland, through the project No. 2017/27/B/ST4/02739. Computations presented in this research were carried out with the support of the Interdisciplinary Center for Mathematical and Computational Modeling (ICM) at the University of Warsaw, grant numbers G86-1021 and G88-1217.

Supporting Information Available

The following file is available free of charge via the Internet at <http://pubs.acs.org>:

- `quad-supp.pdf`: additional derivations and technical details of the proposed computational procedure;
- `geometries.tar`: optimized molecular geometries from Sec. 3.3 in the `*.xyz` format.

References

- (1) Kolda, T. G.; Bader, B. W. Tensor Decompositions and Applications. *SIAM Review* **2009**, *51*, 455–500.
- (2) Hohenstein, E. G.; Parrish, R. M.; Martínez, T. J. Tensor hypercontraction density fitting. I. Quartic scaling second- and third-order Møller-Plesset perturbation theory. *J. Chem. Phys.* **2012**, *137*, 044103.
- (3) Parrish, R. M.; Hohenstein, E. G.; Martínez, T. J.; Sherrill, C. D. Tensor hypercontraction. II. Least-squares renormalization. *J. Chem. Phys.* **2012**, *137*, 224106.
- (4) Parrish, R. M.; Hohenstein, E. G.; Schunck, N. F.; Sherrill, C. D.; Martínez, T. J. Exact Tensor Hypercontraction: A Universal Technique for the Resolution of Matrix Elements of Local Finite-Range N -Body Potentials in Many-Body Quantum Problems. *Phys. Rev. Lett.* **2013**, *111*, 132505.
- (5) Parrish, R. M.; Hohenstein, E. G.; Martínez, T. J.; Sherrill, C. D. Discrete variable representation in electronic structure theory: Quadrature grids for least-squares tensor hypercontraction. *J. Chem. Phys.* **2013**, *138*, 194107.
- (6) Kinoshita, T.; Hino, O.; Bartlett, R. J. Singular value decomposition approach for the approximate coupled-cluster method. *J. Chem. Phys.* **2003**, *119*, 7756–7762.
- (7) Benedikt, U.; Böhm, K.-H.; Auer, A. A. Tensor decomposition in post-Hartree-Fock methods. II. CCD implementation. *J. Chem. Phys.* **2013**, *139*, 224101.

(8) Hohenstein, E. G.; Kokkila, S. I. L.; Parrish, R. M.; Martínez, T. J. Quartic scaling second-order approximate coupled cluster singles and doubles via tensor hypercontraction: THC-CC2. *J. Chem. Phys.* **2013**, *138*, 124111.

(9) Shenvi, N.; van Aggelen, H.; Yang, Y.; Yang, W. Tensor hypercontracted ppRPA: Reducing the cost of the particle-particle random phase approximation from $O(r^6)$ to $O(r^4)$. *J. Chem. Phys.* **2014**, *141*, 024119.

(10) Kokkila Schumacher, S. I. L.; Hohenstein, E. G.; Parrish, R. M.; Wang, L.-P.; Martínez, T. J. Tensor Hypercontraction Second-Order Møller-Plesset Perturbation Theory: Grid Optimization and Reaction Energies. *J. Chem. Theory Comput.* **2015**, *11*, 3042–3052.

(11) Lesiuk, M. Efficient singular-value decomposition of the coupled-cluster triple excitation amplitudes. *J. Comp. Chem.* **2019**, *40*, 1319–1332.

(12) Parrish, R. M.; Zhao, Y.; Hohenstein, E. G.; Martínez, T. J. Rank reduced coupled cluster theory. I. Ground state energies and wavefunctions. *J. Chem. Phys.* **2019**, *150*, 164118.

(13) Lee, J.; Lin, L.; Head-Gordon, M. Systematically Improvable Tensor Hypercontraction: Interpolative Separable Density-Fitting for Molecules Applied to Exact Exchange, Second- and Third-Order Møller-Plesset Perturbation Theory. *J. Chem. Theory Comput.* **2020**, *16*, 243–263.

(14) Lesiuk, M. Implementation of the Coupled-Cluster Method with Single, Double, and Triple Excitations using Tensor Decompositions. *J. Chem. Theory Comput.* **2020**, *16*, 453–467.

(15) Matthews, D. A. A critical analysis of least-squares tensor hypercontraction applied to MP3. *J. Chem. Phys.* **2021**, *154*, 134102.

(16) Lesiuk, M. Near-Exact CCSDT Energetics from Rank-Reduced Formalism Supplemented by Non-iterative Corrections. *J. Chem. Theory Comput.* **2021**, *17*, 7632–7647.

(17) Lesiuk, M. Quintic-scaling rank-reduced coupled cluster theory with single and double excitations. *J. Chem. Phys.* **2022**, *156*, 064103.

(18) Crawford, T. D.; Schaefer III, H. F. *Rev. Comp. Chem.*; John Wiley & Sons, Ltd, 2007; pp 33–136.

(19) Bartlett, R. J.; Musiał, M. Coupled-cluster theory in quantum chemistry. *Rev. Mod. Phys.* **2007**, *79*, 291–352.

(20) Noga, J.; Bartlett, R. J. The full CCSDT model for molecular electronic structure. *J. Chem. Phys.* **1987**, *86*, 7041–7050.

(21) Scuseria, G. E.; Schaefer, H. F. A new implementation of the full CCSDT model for molecular electronic structure. *Chem. Phys. Lett.* **1988**, *152*, 382 – 386.

(22) Tucker, L. R. Some mathematical notes on three-mode factor analysis. *Psychometrika* **1966**, *31*, 279–311.

(23) De Lathauwer, L.; De Moor, B.; Vandewalle, J. A Multilinear Singular Value Decomposition. *SIAM J. Matrix Anal. Appl.* **2000**, *21*, 1253–1278.

(24) Gauss, J.; Stanton, J. F. Analytic gradients for the coupled-cluster singles, doubles, and triples (CCSDT) model. *J. Chem. Phys.* **2002**, *116*, 1773–1782.

(25) Řezáč, J.; Šimová, L.; Hobza, P. CCSD[T] Describes Noncovalent Interactions Better than the CCSD(T), CCSD(TQ), and CCSDT Methods. *J. Chem. Theory Comput.* **2013**, *9*, 364–369.

(26) Šimová, L.; Řezáč, J.; Hobza, P. Convergence of the Interaction Energies in Noncovalent Complexes in the Coupled-Cluster Methods Up to Full Configuration Interaction. *J. Chem. Theory Comput.* **2013**, *9*, 3420–3428.

(27) Smith, D. G. A.; Jankowski, P.; Slawik, M.; Witek, H. A.; Patkowski, K. Basis Set Convergence of the Post-CCSD(T) Contribution to Noncovalent Interaction Energies. *J. Chem. Theory Comput.* **2014**, *10*, 3140–3150.

(28) Karton, A. Highly Accurate CCSDT(Q)/CBS Reaction Barrier Heights for a Diverse Set of Transition Structures: Basis Set Convergence and Cost-Effective Approaches for Estimating Post-CCSD(T) Contributions. *J. Phys. Chem. A* **2019**, *123*, 6720–6732.

(29) Kodrycka, M.; Patkowski, K. Platinum, gold, and silver standards of intermolecular interaction energy calculations. *J. Chem. Phys.* **2019**, *151*, 070901.

(30) Kucharski, S. A.; Bartlett, R. J. Recursive intermediate factorization and complete computational linearization of the coupled-cluster single, double, triple, and quadruple excitation equations. *Theor. Chim. Acta* **1991**, *80*, 387–405.

(31) Oliphant, N.; Adamowicz, L. Coupled-cluster method truncated at quadruples. *J. Chem. Phys.* **1991**, *95*, 6645–6651.

(32) Kucharski, S. A.; Bartlett, R. J. The coupled-cluster single, double, triple, and quadruple excitation method. *J. Chem. Phys.* **1992**, *97*, 4282–4288.

(33) Kucharski, S. A.; Musiał, M. Connected quadruple excitations in the coupled-cluster theory. *Mol. Phys.* **2010**, *108*, 2975–2985.

(34) Bartlett, R. J.; Watts, J.; Kucharski, S.; Noga, J. Non-iterative fifth-order triple and quadruple excitation energy corrections in correlated methods. *Chem. phys. lett.* **1990**, *165*, 513–522.

(35) Kucharski, S. A.; Bartlett, R. J. An efficient way to include connected quadruple contributions into the coupled cluster method. *J. Chem. Phys.* **1998**, *108*, 9221–9226.

(36) Kucharski, S. A.; Bartlett, R. J. Noniterative energy corrections through fifth-order to the coupled cluster singles and doubles method. *J. Chem. Phys.* **1998**, *108*, 5243–5254.

(37) Bomble, Y. J.; Stanton, J. F.; Kállay, M.; Gauss, J. Coupled-cluster methods including noniterative corrections for quadruple excitations. *J. Chem. Phys.* **2005**, *123*, 054101.

(38) Kállay, M.; Gauss, J. Approximate treatment of higher excitations in coupled-cluster theory. *J. Chem. Phys.* **2005**, *123*, 214105.

(39) Kállay, M.; Gauss, J. Approximate treatment of higher excitations in coupled-cluster theory. II. Extension to general single-determinant reference functions and improved approaches for the canonical Hartree-Fock case. *J. Chem. Phys.* **2008**, *129*, 144101.

(40) Eriksen, J. J.; Jørgensen, P.; Olsen, J.; Gauss, J. Equation-of-motion coupled cluster perturbation theory revisited. *J. Chem. Phys.* **2014**, *140*, 174114.

(41) Eriksen, J.; Kristensen, K.; Kjærgaard, T.; Jørgensen, P.; Gauss, J. A Lagrangian framework for deriving triples and quadruples corrections to the CCSD energy. *J. Chem. Phys.* **2014**, *140*, 064108.

(42) De Lathauwer, L.; De Moor, B.; Vandewalle, J. On the Best Rank-1 and Rank- (R_1, R_2, \dots, R_N) Approximation of Higher-Order Tensors. *SIAM J. Matrix Anal. Appl.* **2000**, *21*, 1324–1342.

(43) Eldén, L.; Savas, B. A Newton–Grassmann Method for Computing the Best Multi-linear Rank- (r_1, r_2, r_3) Approximation of a Tensor. *SIAM J. Matrix Anal. Appl.* **2009**, *31*, 248–271.

(44) Eriksen, J. J.; Matthews, D. A.; Jørgensen, P.; Gauss, J. Communication: The performance of non-iterative coupled cluster quadruples models. *J. Chem. Phys.* **2015**, *143*, 041101.

(45) Paldus, J.; Jeziorski, B. Clifford algebra and unitary group formulations of the many-electron problem. *Theor. Chem. Acc.* **1988**, *73*, 81–103.

(46) Whitten, J. L. Coulombic potential energy integrals and approximations. *J. Chem. Phys.* **1973**, *58*, 4496–4501.

(47) Baerends, E.; Ellis, D.; Ros, P. Self-consistent molecular Hartree-Fock-Slater calculations I. The computational procedure. *Chem. Phys.* **1973**, *2*, 41 – 51.

(48) Dunlap, B. I.; Connolly, J. W. D.; Sabin, J. R. On some approximations in applications of $X\alpha$ theory. *J. Chem. Phys.* **1979**, *71*, 3396–3402.

(49) Van Alsenoy, C. Ab initio calculations on large molecules: The multiplicative integral approximation. *J. Comp. Chem.* **1988**, *9*, 620–626.

(50) Vahtras, O.; Almlöf, J.; Feyereisen, M. Integral approximations for LCAO-SCF calculations. *Chem. Phys. Lett.* **1993**, *213*, 514 – 518.

(51) DePrince, A. E.; Sherrill, C. D. Accuracy and Efficiency of Coupled-Cluster Theory Using Density Fitting/Cholesky Decomposition, Frozen Natural Orbitals, and a t1-Transformed Hamiltonian. *J. Chem. Theory Comp.* **2013**, *9*, 2687–2696.

(52) Lesiuk, M. A straightforward a posteriori method for reduction of density-fitting error in coupled-cluster calculations. *J. Chem. Phys.* **2020**, *152*, 044104.

(53) Kucharski, S. A.; Bartlett, R. J. In *Fifth-Order Many-Body Perturbation Theory and Its Relationship to Various Coupled-Cluster Approaches*; Löwdin, P.-O., Ed.; Adv. Quantum Chem.; Academic Press, 1986; Vol. 18; pp 281–344.

(54) Kucharski, S. A.; Bartlett, R. J. Coupled-cluster methods that include connected quadruple excitations, T4: CCSDTQ-1 and Q(CCSDT). *Chem. Phys. Lett.* **1989**, *158*, 550–555.

(55) Kucharski, S. A.; Noga, J.; Bartlett, R. J. Fifth-order many-body perturbation theory for molecular correlation energies. *J. Chem. Phys.* **1989**, *90*, 7282–7290.

(56) Noga, J.; Kucharski, S. A.; Bartlett, R. J. A coupled-cluster method that includes connected quadruple excitations. *J. Chem. Phys.* **1989**, *90*, 3399–3400.

(57) Stanton, J. F.; Bartlett, R. J. The equation of motion coupled-cluster method. A systematic biorthogonal approach to molecular excitation energies, transition probabilities, and excited state properties. *J. Chem. Phys.* **1993**, *98*, 7029–7039.

(58) Frantz, L. M.; Mills, R. L. Many-body basis for the optical model. *Nucl. Phys.* **1960**, *15*, 16–32.

(59) Kowalski, K.; Piecuch, P. The method of moments of coupled-cluster equations and the renormalized CCSD[T], CCSD(T), CCSD(TQ), and CCSDT(Q) approaches. *J. Chem. Phys.* **2000**, *113*, 18–35.

(60) Piecuch, P.; Kowalski, K.; Pimienta, I. S. O.; McGuire, M. J. Recent advances in electronic structure theory: Method of moments of coupled-cluster equations and renormalized coupled-cluster approaches. *Int. Rev. Phys. Chem.* **2002**, *21*, 527–655.

(61) Piecuch, P.; Kowalski, K.; Pimienta, I. S. O.; Fan, P.-D.; Lodriguito, M.; McGuire, M. J.; Kucharski, S. A.; Kuś, T.; Musiał, M. Method of moments of coupled-cluster equations: a new formalism for designing accurate electronic structure methods for ground and excited states. *Theor. Chem. Acc.* **2004**, *112*, 349–393.

(62) Piecuch, P.; Włoch, M. Renormalized coupled-cluster methods exploiting left eigenstates of the similarity-transformed Hamiltonian. *J. Chem. Phys.* **2005**, *123*, 224105.

(63) Sun, Y.; Huang, K. HOQRI: Higher-Order QR Iteration for Scalable Tucker Decomposition. ICASSP 2022 - 2022 IEEE International Conference on Acoustics, Speech and Signal Processing (ICASSP). 2022; pp 3648–3652.

(64) Almlöf, J. Elimination of energy denominators in Møller-Plesset perturbation theory by a Laplace transform approach. *Chem. Phys. Lett.* **1991**, *181*, 319 – 320.

(65) Häser, M.; Almlöf, J. Laplace transform techniques in Møller-Plesset perturbation theory. *J. Chem. Phys.* **1992**, *96*, 489–494.

(66) Ayala, P. Y.; Scuseria, G. E. Linear scaling second-order Møller-Plesset theory in the atomic orbital basis for large molecular systems. *J. Chem. Phys.* **1999**, *110*, 3660–3671.

(67) Lambrecht, D. S.; Doser, B.; Ochsenfeld, C. Rigorous integral screening for electron correlation methods. *J. Chem. Phys.* **2005**, *123*, 184102.

(68) Nakajima, T.; Hirao, K. An approximate second-order Møller-Plesset perturbation approach for large molecular calculations. *Chem. Phys. Lett.* **2006**, *427*, 225 – 229.

(69) Jung, Y.; Lochan, R. C.; Dutoi, A. D.; Head-Gordon, M. Scaled opposite-spin second order Møller-Plesset correlation energy: An economical electronic structure method. *J. Chem. Phys.* **2004**, *121*, 9793–9802.

(70) Kats, D.; Usyat, D.; Schütz, M. On the use of the Laplace transform in local correlation methods. *Phys. Chem. Chem. Phys.* **2008**, *10*, 3430–3439.

(71) Takatsuka, A.; Ten-no, S.; Hackbusch, W. Minimax approximation for the decomposition of energy denominators in Laplace-transformed Møller-Plesset perturbation theories. *J. Chem. Phys.* **2008**, *129*, 044112.

(72) Braess, D.; Hackbusch, W. Approximation of $1/x$ by exponential sums in $[1, \infty)$. *IMA J. Numer. Anal.* **2005**, *25*, 685–697.

(73) Helmich-Paris, B.; Visscher, L. Improvements on the minimax algorithm for the Laplace transformation of orbital energy denominators. *J. Comp. Phys.* **2016**, *321*, 927 – 931.

(74) Dunning, T. H. Gaussian basis sets for use in correlated molecular calculations. I. The atoms boron through neon and hydrogen. *J. Chem. Phys.* **1989**, *90*, 1007–1023.

(75) Weigend, F.; Köhn, A.; Hättig, C. Efficient use of the correlation consistent basis sets in resolution of the identity MP2 calculations. *The Journal of Chemical Physics* **2002**, *116*, 3175–3183.

(76) Hättig, C. Optimization of auxiliary basis sets for RI-MP2 and RI-CC2 calculations: Core-valence and quintuple- ζ basis sets for H to Ar and QZVPP basis sets for Li to Kr. *Phys. Chem. Chem. Phys.* **2005**, *7*, 59–66.

(77) Stanton, J. F.; Gauss, J.; Cheng, L.; Harding, M. E.; Matthews, D. A.; Szalay, P. G. CFOUR, Coupled-Cluster techniques for Computational Chemistry, a quantum-chemical program package. With contributions from A.A. Auer, R.J. Bartlett, U. Benedikt, C. Berger, D.E. Bernholdt, S. Blaschke, Y. J. Bomble, S. Burger, O. Christiansen, D. Datta, F. Engel, R. Faber, J. Greiner, M. Heckert, O. Heun, M. Hilgenberg, C. Huber, T.-C. Jagau, D. Jonsson, J. Jusélius, T. Kirsch, K. Klein, G.M. KopperW.J. Lauderdale, F. Lipparini, T. Metzroth, L.A. Mück, D.P. O'Neill, T. Nottoli, D.R. Price, E. Prochnow, C. Puzzarini, K. Ruud, F. Schiffmann, W. Schwalbach, C. Simmons, S. Stopkowicz, A. Tajti, J. Vázquez, F. Wang, J.D. Watts and the integral packages MOLECULE (J. Almlöf and P.R. Taylor), PROPS (P.R. Taylor), ABACUS (T. Helgaker, H.J. Aa. Jensen, P. Jørgensen, and J. Olsen), and ECP routines by A. V. Mitin and C. van Wüllen. For the current version, see <http://www.cfour.de>.

(78) Matthews, D. A.; Cheng, L.; Harding, M. E.; Lipparini, F.; Stopkowicz, S.; Jagau, T.-C.; Szalay, P. G.; Gauss, J.; Stanton, J. F. Coupled-cluster techniques for computational chemistry: The CFOUR program package. *J. Chem. Phys.* **2020**, *152*, 214108.

(79) Aprà, E.; Bylaska, E. J.; de Jong, W. A.; Govind, N.; Kowalski, K.; Straatsma, T. P.; Valiev, M.; van Dam, H. J. J.; Alexeev, Y.; Anchell, J.; Anisimov, V.; Aquino, F. W.; Atta-Fynn, R.; Autschbach, J.; Bauman, N. P.; Becca, J. C.; Bernholdt, D. E.; Bhaskaran-Nair, K.; Bogatko, S.; Borowski, P.; Boschen, J.; Brabec, J.; Bruner, A.; Cauët, E.; Chen, Y.; Chuev, G. N.; Cramer, C. J.; Daily, J.; Deegan, M. J. O.;

Dunning, T. H.; Dupuis, M.; Dyall, K. G.; Fann, G. I.; Fischer, S. A.; Fonari, A.; Früchtl, H.; Gagliardi, L.; Garza, J.; Gawande, N.; Ghosh, S.; Glaesemann, K.; Götz, A. W.; Hammond, J.; Helms, V.; Hermes, E. D.; Hirao, K.; Hirata, S.; Jacquelin, M.; Jensen, L.; Johnson, B. G.; Jónsson, H.; Kendall, R. A.; Klemm, M.; Kobayashi, R.; Konkov, V.; Krishnamoorthy, S.; Krishnan, M.; Lin, Z.; Lins, R. D.; Littlefield, R. J.; Logsdail, A. J.; Lopata, K.; Ma, W.; Marenich, A. V.; Martin del Campo, J.; Mejia-Rodriguez, D.; Moore, J. E.; Mullin, J. M.; Nakajima, T.; Nascimento, D. R.; Nichols, J. A.; Nichols, P. J.; Nieplocha, J.; Otero-de-la Roza, A.; Palmer, B.; Panyala, A.; Pirojsirikul, T.; Peng, B.; Peverati, R.; Pittner, J.; Pollack, L.; Richard, R. M.; Sadayappan, P.; Schatz, G. C.; Shelton, W. A.; Silverstein, D. W.; Smith, D. M. A.; Soares, T. A.; Song, D.; Swart, M.; Taylor, H. L.; Thomas, G. S.; Tippuraju, V.; Truhlar, D. G.; Tsemekhman, K.; Van Voorhis, T.; Vázquez-Mayagoitia, A.; Verma, P.; Villa, O.; Vishnu, A.; Vogiatzis, K. D.; Wang, D.; Weare, J. H.; Williamson, M. J.; Windus, T. L.; Woliński, K.; Wong, A. T.; Wu, Q.; Yang, C.; Yu, Q.; Zacharias, M.; Zhang, Z.; Zhao, Y.; Harrison, R. J. NWChem: Past, present, and future. *J. Chem. Phys.* **2020**, *152*, 184102.

(80) Matthews, D. A. High-Performance Tensor Contraction without Transposition. *SIAM J. Sci. Comput.* **2018**, *40*, C1–C24.

(81) Gyevi-Nagy, L.; Kállay, M.; Nagy, P. R. Accurate Reduced-Cost CCSD(T) Energies: Parallel Implementation, Benchmarks, and Large-Scale Applications. *J. Chem. Theory Comp.* **2021**, *17*, 860–878.

(82) Jones, R. R.; Bergman, R. G. p-Benzyne. Generation as an intermediate in a thermal isomerization reaction and trapping evidence for the 1, 4-benzenediyl structure. *J. Am. Chem. Soc.* **1972**, *94*, 660–661.

(83) Wenthold, P. G.; Squires, R. R.; Lineberger, W. C. Ultraviolet Photoelectron Spec-

troscopy of the o-, m-, and p-Benzyne Negative Ions. Electron Affinities and Singlet-Triplet Splittings for o-, m-, and p-Benzynes. *J. Am. Chem. Soc.* **1998**, *120*, 5279–5290.

(84) Lindh, R.; Lee, T. J.; Bernhardsson, A.; Persson, B. J.; Karlstroem, G. Extended ab initio and theoretical thermodynamics studies of the Bergman reaction and the energy splitting of the singlet o-, m-, and p-benzynes. *J. Am. Chem. Soc.* **1995**, *117*, 7186–7194.

(85) Cramer, C. J.; Nash, J. J.; Squires, R. R. A reinvestigation of singlet benzene thermochemistry predicted by CASPT2, coupled-cluster and density functional calculations. *Chem. Phys. Lett.* **1997**, *277*, 311–320.

(86) Lindh, R.; Bernhardsson, A.; Schütz, M. Benzene Thermochemistry: A Benchmark ab Initio Study. *J. Phys. Chem. A* **1999**, *103*, 9913–9920.

(87) V. Moskaleva, L.; K. Madden, L.; C. Lin, M. Unimolecular isomerization/decomposition of ortho-benzene: ab initio MO/statistical theory study. *Phys. Chem. Chem. Phys.* **1999**, *1*, 3967–3972.

(88) Crawford, T. D.; Kraka, E.; Stanton, J. F.; Cremer, D. Problematic p-benzene: Orbital instabilities, biradical character, and broken symmetry. *J. Chem. Phys.* **2001**, *114*, 10638–10650.

(89) Smith, C. E.; Crawford, T. D.; Cremer, D. The structures of m-benzene and tetrafluoro-m-benzene. *J. Chem. Phys.* **2005**, *122*, 174309.

(90) Karton, A.; Kaminker, I.; Martin, J. M. L. Economical Post-CCSD(T) Computational Thermochemistry Protocol and Applications to Some Aromatic Compounds. *J. Phys. Chem. A* **2009**, *113*, 7610–7620.

(91) Ghigo, G.; Maranzana, A.; Tonachini, G. o-Benzene fragmentation and isomerization pathways: a CASPT2 study. *Phys. Chem. Chem. Phys.* **2014**, *16*, 23944–23951.

(92) Tadross, P. M.; Stoltz, B. M. *Chem. Rev.* **2012**, *112*, 3550–3577.

(93) Hirsch, F.; Reusch, E.; Constantinidis, P.; Fischer, I.; Bakels, S.; Rijs, A. M.; Hemberger, P. *J. Phys. Chem. A* **2018**, *122*, 9563–9571.

(94) Crews, P.; Beard, J. Cycloadditions of benzyne with cyclic olefins. Competition between $2 + 4$, ene, and $2 + 2$ reaction pathways. *J. Org. Chem.* **1973**, *38*, 522–528.

(95) Matsugi, A.; Miyoshi, A. Reactions of o-benzyne with propargyl and benzyl radicals: potential sources of polycyclic aromatic hydrocarbons in combustion. *Phys. Chem. Chem. Phys.* **2012**, *14*, 9722–9728.

(96) Martínez, J. P.; Langa, F.; Bickelhaupt, F. M.; Osuna, S.; Solà, M. (4 + 2) and (2 + 2) Cycloadditions of Benzyne to C_{60} and Zig-Zag Single-Walled Carbon Nanotubes: The Effect of the Curvature. *J. Phys. Chem. C* **2016**, *120*, 1716–1726.

(97) Curtiss, L. A.; Jones, C.; Trucks, G. W.; Raghavachari, K.; Pople, J. A. Gaussian-1 theory of molecular energies for second-row compounds. *J. Chem. Phys.* **1990**, *93*, 2537–2545.

(98) Curtiss, L. A.; Raghavachari, K.; Trucks, G. W.; Pople, J. A. Gaussian-2 theory for molecular energies of first- and second-row compounds. *J. Chem. Phys.* **1991**, *94*, 7221–7230.

(99) Curtiss, L. A.; Raghavachari, K.; Redfern, P. C.; Rassolov, V.; Pople, J. A. Gaussian-3 (G3) theory for molecules containing first and second-row atoms. *J. Chem. Phys.* **1998**, *109*, 7764–7776.

(100) Curtiss, L. A.; Redfern, P. C.; Raghavachari, K. Gaussian-4 theory. *J. Chem. Phys.* **2007**, *126*, 084108.

(101) Martin, J. M. L.; de Oliveira, G. Towards standard methods for benchmark quality ab initio thermochemistry – W1 and W2 theory. *J. Chem. Phys.* **1999**, *111*, 1843–1856.

(102) Boese, A. D.; Oren, M.; Atasoylu, O.; Martin, J. M. L.; Kállay, M.; Gauss, J. W3 theory: Robust computational thermochemistry in the kJ/mol accuracy range. *J. Chem. Phys.* **2004**, *120*, 4129–4141.

(103) Karton, A.; Rabinovich, E.; Martin, J. M. L.; Ruscic, B. W4 theory for computational thermochemistry: In pursuit of confident sub-kJ/mol predictions. *J. Chem. Phys.* **2006**, *125*, 144108.

(104) Tajti, A.; Szalay, P. G.; Császár, A. G.; Kállay, M.; Gauss, J.; Valeev, E. F.; Flowers, B. A.; Vázquez, J.; Stanton, J. F. HEAT: High accuracy extrapolated ab initio thermochemistry. *J. Chem. Phys.* **2004**, *121*, 11599–11613.

(105) Bomble, Y. J.; Vázquez, J.; Kállay, M.; Michauk, C.; Szalay, P. G.; Császár, A. G.; Gauss, J.; Stanton, J. F. High-accuracy extrapolated ab initio thermochemistry. II. Minor improvements to the protocol and a vital simplification. *J. Chem. Phys.* **2006**, *125*, 064108.

(106) Harding, M. E.; Vázquez, J.; Ruscic, B.; Wilson, A. K.; Gauss, J.; Stanton, J. F. High-accuracy extrapolated ab initio thermochemistry. III. Additional improvements and overview. *J. Chem. Phys.* **2008**, *128*, 114111.

(107) Lesiuk, M.; Jeziorski, B. Complete Basis Set Extrapolation of Electronic Correlation Energies Using the Riemann Zeta Function. *J. Chem. Theory Comput.* **2019**, *15*, 5398–5403.

(108) Czachorowski, P.; Przybytek, M.; Lesiuk, M.; Puchalski, M.; Jeziorski, B. Second virial coefficients for ${}^4\text{He}$ and ${}^3\text{He}$ from an accurate relativistic interaction potential. *Phys. Rev. A* **2020**, *102*, 042810.

(109) Sinha, P.; Boesch, S. E.; Gu, C.; Wheeler, R. A.; Wilson, A. K. Harmonic Vibrational Frequencies: Scaling Factors for HF, B3LYP, and MP2 Methods in Combination with Correlation Consistent Basis Sets. *J. Phys. Chem. A* **2004**, *108*, 9213–9217.

(110) Vosko, S. H.; Wilk, L.; Nusair, M. Accurate spin-dependent electron liquid correlation energies for local spin density calculations: a critical analysis. *Can. J. Phys.* **1980**, *58*, 1200–1211.

(111) Lee, C.; Yang, W.; Parr, R. G. Development of the Colle-Salvetti correlation-energy formula into a functional of the electron density. *Phys. Rev. B* **1988**, *37*, 785–789.

(112) Becke, A. D. A new mixing of Hartree–Fock and local density-functional theories. *J. Chem. Phys.* **1993**, *98*, 1372–1377.

(113) Stephens, P. J.; Devlin, F. J.; Chabalowski, C. F.; Frisch, M. J. Ab initio calculation of vibrational absorption and circular dichroism spectra using density functional force fields. *J. Phys. Chem.* **1994**, *98*, 11623–11627.

(114) Bakowies, D.; von Lilienfeld, O. A. Density Functional Geometries and Zero-Point Energies in Ab Initio Thermochemical Treatments of Compounds with First-Row Atoms (H, C, N, O, F). *J. Chem. Theory Comput.* **2021**, *17*, 4872–4890.

(115) Johnson, R. D., et al. NIST computational chemistry comparison and benchmark database. <http://srdatal.nist.gov/cccbdb> **2020**, Release 21, August 2020, <http://cccbdb.nist.gov/>.

(116) Mebel, A. M.; Morokuma, K.; Lin, M. C. Modification of the gaussian-2 theoretical model: The use of coupled-cluster energies, density-functional geometries, and frequencies. *J. Chem. Phys.* **1995**, *103*, 7414–7421.

(117) Peterson, K. A.; Dunning, T. H. Accurate correlation consistent basis sets for molecular core–valence correlation effects: The second row atoms Al–Ar, and the first row atoms B–Ne revisited. *J. Chem. Phys.* **2002**, *117*, 10548–10560.

(118) Douglas, M.; Kroll, N. M. Quantum electrodynamical corrections to the fine structure of helium. *Ann. Phys.* **1974**, *82*, 89–155.

(119) Hess, B. A. Applicability of the no-pair equation with free-particle projection operators to atomic and molecular structure calculations. *Phys. Rev. A* **1985**, *32*, 756–763.

(120) Reiher, M. Douglas–Kroll–Hess Theory: a relativistic electrons-only theory for chemistry. *Theor. Chem. Acc.* **2006**, *116*, 241–252.

(121) de Jong, W. A.; Harrison, R. J.; Dixon, D. A. Parallel Douglas–Kroll energy and gradients in NWChem: Estimating scalar relativistic effects using Douglas–Kroll contracted basis sets. *J. Chem. Phys.* **2001**, *114*, 48–53.

(122) Gauss, J.; Tajti, A.; Kállay, M.; Stanton, J. F.; Szalay, P. G. Analytic calculation of the diagonal Born–Oppenheimer correction within configuration-interaction and coupled-cluster theory. *J. Chem. Phys.* **2006**, *125*, 144111.

(123) Ault, A. The Bullvalene Story. The Conception of Bullvalene, a Molecule That Has No Permanent Structure. *J. Chem. Ed.* **2001**, *78*, 924.

(124) von E. Doering, W.; Roth, W. A rapidly reversible degenerate cope rearrangement: Bicyclo[5.1.0]octa-2,5-diene. *Tetrahedron* **1963**, *19*, 715–737.

(125) Schröder, G. Preparation and Properties of Tricyclo[3,3,2,0^{4,6}]deca-2,7,9-triene (Bullvalene). *Angew. Chem. Int. Ed. Engl.* **1963**, *2*, 481–482.

(126) Karton, A. Cope rearrangements in shapeshifting molecules re-examined by means of high-level CCSDT(Q) composite ab initio methods. *Chem. Phys. Lett.* **2020**, *759*, 138018.

(127) Moreno, P. O.; Suarez, C.; Tafazzoli, M.; True, N. S.; LeMaster, C. B. Gas phase NMR study of the degenerate Cope rearrangement of bullvalene. *J. Phys. Chem.* **1992**, *96*, 10206–10212.

(128) Grimme, S.; Antony, J.; Ehrlich, S.; Krieg, H. A consistent and accurate ab initio

parametrization of density functional dispersion correction (DFT-D) for the 94 elements H–Pu. *J. Chem. Phys.* **2010**, *132*, 154104.

(129) Grimme, S.; Ehrlich, S.; Goerigk, L. Effect of the damping function in dispersion corrected density functional theory. *J. Comp. Chem.* **2011**, *32*, 1456–1465.

(130) Jensen, F. Polarization consistent basis sets: Principles. *J. Chem. Phys.* **2001**, *115*, 9113–9125.

(131) Jensen, F. Polarization consistent basis sets. II. Estimating the Kohn–Sham basis set limit. *J. Chem. Phys.* **2002**, *116*, 7372–7379.

(132) Hanson-Heine, M. W. D. Benchmarking DFT-D Dispersion Corrections for Anharmonic Vibrational Frequencies and Harmonic Scaling Factors. *J. Phys. Chem. A* **2019**, *123*, 9800–9808.

(133) Hrovat, D. A.; Brown, E. C.; Williams, R. V.; Quast, H.; Borden, W. T. How Important Is Bishomoaromatic Stabilization in Determining the Relative Barrier Heights for the Degenerate Cope Rearrangements of Semibullvalene, Barbaralane, Bullvalene, and Dihydrobullvalene? *J. Org. Chem.* **2005**, *70*, 2627–2632.

(134) Brown, E. C.; Bader, R. F. W.; Werstiuk, N. H. QTAIM Study on the Degenerate Cope Rearrangements of 1,5-Hexadiene and Semibullvalene. *J. Phys. Chem. A* **2009**, *113*, 3254–3265.

(135) Greve, D. R. Homoaromaticity in aza- and phosphasemibullvalenes. A computational study. *J. Phys. Org. Chem.* **2011**, *24*, 222–228.

(136) Khojandi, M.; Seif, A.; Zahedi, E.; Domingo, L. R.; Karimkhani, M. Unravelling the kinetics and molecular mechanism of the degenerate Cope rearrangement of bullvalene. *New J. Chem.* **2020**, *44*, 6543–6552.

(137) Stanton, J. F. On the extent of spin contamination in open-shell coupled-cluster wave functions. *J. Chem. Phys.* **1994**, *101*, 371–374.

(138) Krylov, A. I. Spin-contamination of coupled-cluster wave functions. *J. Chem. Phys.* **2000**, *113*, 6052–6062.

(139) Kitsaras, M.-P.; Stopkowicz, S. Spin contamination in MP2 and CC2, a surprising issue. *J. Chem. Phys.* **2021**, *154*, 131101.

(140) Rittby, M.; Bartlett, R. J. An open-shell spin-restricted coupled cluster method: application to ionization potentials in nitrogen. *J. Chem. Phys.* **1988**, *92*, 3033–3036.

(141) Knowles, P. J.; Hampel, C.; Werner, H. Coupled cluster theory for high spin, open shell reference wave functions. *J. Chem. Phys.* **1993**, *99*, 5219–5227.

(142) Jeziorski, B.; Paldus, J.; Jankowski, P. Unitary group approach to spin-adapted open-shell coupled cluster theory. *Int. J. Quantum Chem.* **1995**, *56*, 129–155.

(143) Crawford, T. D.; Lee, T. J.; Schaefer, H. F. A new spin-restricted triple excitation correction for coupled cluster theory. *J. Chem. Phys.* **1997**, *107*, 7943–7950.

(144) Szalay, P. G.; Gauss, J. Spin-restricted open-shell coupled-cluster theory. *J. Chem. Phys.* **1997**, *107*, 9028–9038.

(145) Jankowski, P.; Jeziorski, B. Unitary group based open-shell coupled cluster theory: Application to van der Waals interactions of high-spin systems. *J. Chem. Phys.* **1999**, *111*, 1857–1869.

(146) Heckert, M.; Heun, O.; Gauss, J.; Szalay, P. G. Towards a spin-adapted coupled-cluster theory for high-spin open-shell states. *J. Chem. Phys.* **2006**, *124*, 124105.

Graphical TOC Entry

